Part III

Material properties

10
Fibers

X-Q. DAI
Soochow University, China

10.1 Textile fibers

A fiber is a unit of matter with an extremely small diameter and a length at least 100 times longer than its width. There are many fibrous substances. Fibers, that are too fine or too short are difficult to process into yarn. And if they are too coarse and thick, they are uncomfortable if worn next to the skin. Therefore, only the fibers having a minimum length (about ½ inch, or 15 millimeters) and a width range (0.0004 – 0.002 inch, or 10–50 micrometers) can be used as textile materials. Historically, natural fibers were the first textile fibers.

10.1.1 Natural fibers

Wool

Wool refers to fibers from sheep, goats, camels, oxen, and fur-bearing animals. Wool was one of the first fibers to be spun into yarn and woven into fabric. Wool fibers are composed of a protein polymer called keratin. A wool fiber is generally crimped three dimensionally. The crimp ranges from 4 to 10 crimps/cm. The fiber length of wool used for apparel products ranges from 5 to 12 cm and size varies from 14 to 45 μm.

Sheep's wool is the most important type of wool fiber because it is the most plentiful. Specialty wool fibers from the hair of the camel, alpaca, llama, and vicuna are more costly than sheep's wool. Wool is used in both woven and knitted fabrics. The fabrics drape well and are durable; and are used primarily in luxury sweaters, coats, and suits. They are comfortable under a variety of conditions and retain their good looks during wear and care.

Silk

Silk is a fine, strong, continuous filament produced by the larva of certain insects, especially the silkworm, when constructing their cocoons. It is a

natural protein fiber composed of fibroin. Early in 2640 BC, the ancient Chinese learned how to reel the silk and make it into fabric. The silk industry was then monopolized by China for over 3000 years. Today, major producers of silk are China, India and Japan. There are two main types of silk fiber, cultivated and wild. They differ in diameter, cross-sectional shape, and fine structure. The most important commercial silk is cultivated. Silk is the only natural filament fiber. It is linear. Its length may be up to 600 m, but generally averages 300 m. Silk has a very fine diameter of 12–30 μm.

The beauty and hand of silk and its high cost make is known as a luxury fiber. It remains an important fiber in fashion designers' collections. Silk is extremely versatile and can be used to create a variety of fabrics from sheer, gossamer chiffons to heavy, beautiful brocades and velvets. Silk underwear, socks, and leggings are also popular due to silk's soft hand and other comfortable physical properties.

Cotton

Cotton is a seed hair obtained from the boll of the cotton plant. It is a natural cellulosic fiber composed of polymers forming a highly crystalline structure with numerous strong hydrogen bonds. Cotton cloth was used by the people of ancient China, Egypt, India, Mexico and Peru. Today, cotton is the most important apparel fiber. There are also many varieties of cotton fibers differing in staple, length, diameter and so on. The terms 'Pima', 'Egyptian', and 'Sea island' denote the most commonly used cotton fibers. The staple lengths of cotton range from 0.32 to 6.35 cm, and those of 2.22–3.18 cm are used as textile materials. The diameter of cotton ranges from 12 to 20 μm. The microscopic appearance of cotton fiber is a flat, twisted ribbon in the longitudinal direction, and its cross-section shows a kidney-bean shape. Cotton fabrics are used where comfort is of primary importance and appearance retention is not as important, or where a more casual fabric is acceptable. Cotton is often mixed with other fibers to improve its durability and appearance retention; blends of 60 percent or 70 percent cotton are usual.

Flax and ramie

Flax fiber is obtained from the inner bark of the stem of a plant grown in temperate and subtropical regions of the world. It is a natural, cellulosic, multi-cellular bast fiber. Flax fiber is 10–100 cm in length. Its diameter varies from 40 to 80 μm. Flax is stronger than cotton as its polymers lie almost parallel to the fiber axis. Flax is one of the oldest textile fibers. Fabric made from flax is called linen. Remnants of linen were found among the remains

of the Swiss Lake Dwellers, who lived in 8000 BC; linen mummy cloths more than 3000 years old have been found in Egyptian tombs. Actually, the linen industry flourished in Europe until the 18th century. However, with the invention of power spinning, cotton replaced flax as the most important and widely-used fiber. Today, flax is a prestige fiber as a result of its limited production and relatively high cost. Apparel made of linen is usually designed for warm weather use, high fashion aspects, or professional wear.

Ramie is another common bast fiber. It has been used for several thousand years in China. The ramie plant is a tall perennial shrub from the nettle family that requires a hot, humid climate for growth. It grows primarily in China, the Philippines, and Brazil. Ramie fiber is longer than 150 cm. It is a coarse fiber with a fiber size of 4.6–6.4 denier. Ramie fiber is used in a wide variety of apparel items: sweaters, shirts, blouses, and suits. It is often in blends, particularly with cotton or wool.

10.1.2 Regenerated fibers

Regenerated fibers are manufactured cellulosic fibers. These polymers do not naturally occur as fibers; processing is carried out to convert them into fiber form.

Rayon

Rayon was the first manufactured cellulosic fiber. The development of rayon fiber can be traced back to 1664, when the English physicist Robert Hooke suggested it might be possible to spin artificial filaments from a cellulosic gummy substance resembling the secretion of silkworms. In the next two centuries, several inquisitive scientists tried numerous methods to produce an 'artificial' silk. In 1884 in France, Count Hilaire de Chardonnet, called the 'father of rayon', made the first practical commercial production of rayon fiber. After that, various manufacturing processes were developed for its production.

Rayon fiber is available as filament, staple, and tow. Most rayon is used in staple form. Normally, rayon fibers range from 1.5 to 15 deniers. Observed under a microscope, a regular viscose rayon fiber shows a striated surface and a serrated cross-section. Rayon fiber is a manufactured fiber composed of 100% regenerated cellulose, or regenerated cellulose in which chemical substituents have replaced not more than 15% of the hydrogens of the hydroxyl groups. Rayon fiber is soft, comfortable and versatile. It is mostly used in woven fabrics, which have a unique drape that designers love. It is also used in non-woven fabrics.

Acetate

Acetate is another manufactured cellulosic fiber made from the same raw material as rayon, cellulose, but by a different manufacturing process involving a greater degree of chemical modification. Acetate is available as staple or filament. Observed under a microscope, an acetate fiber shows a striated surface and a lobed cross-section. The appearance of acetate fiber is very similar to that of silk: bright, shiny, and smooth to the eye and hand. The low cost and good draping qualities of acetate make it a valuable and beautiful fiber. An important use of acetate is as a lining fabric; another one is in robes and loungewear. Acetate and also rayon are the two oldest manufactured fibers and have been produced in large quantities, filling an important need for low cost fibers in the textile industry.

10.1.3 Synthetic fibers

Synthetic fibers are non-cellulosic manufactured fibers. In producing synthetic fibers, the fiber-forming compounds must be made from basic raw materials (monomers) by a polymerization process. Different chemical compounds are used as the raw materials to make the polymers for nylon, olefin, and acrylic polymers.

Nylon

Nylon was the first synthetic fiber. It was developed by the Du Pont Company in 1939. Nylon is a manufactured fiber in which the fiber-forming substance is any long-chain synthetic polyamide in which less than 85% of the amide linkages are attached to two aromatic rings. Nylon fiber is highly crystalline, oriented, and strongly hydrogen bonded between two types of polar groups in both the crystalline and amorphous areas. So it is very strong, tough and flexible. Nylon is available in multifilament, monofilament, staple, and tow in a wide range of deniers and shapes. There are many variants of the two commonest types of nylon, nylon 6 and nylon 6,6, altering in fiber denier, cross-section and crimp.

Today, nylon is very successful in hosiery and in knitted-filament fabrics such as tricot and jersey, because of its smoothness, light weight, high strength, and good recovery after high elongation. Nylon is also used for lining fabrics in coats and jackets. These linings are more durable; however, their cost is greater than acetate fabrics. In the apparel markets, most nylon is used in filament form rather than staple.

Polyester

The first viable polyester fiber was produced in England by ICI, and it was introduced to the USA in 1951 by the Du Pont Company. Since then, polyesters have undergone significant research and development work. Today, polyester refers to manufactured fibers in which the fiber-forming substance is any long-chain polymer composed of at least 85% by weight of an ester of a substituted aromatic carboxylic acid, including but not restricted to substituted terephthalate units and parasubstituted hydroxybenzoate units.

Polyester is a highly crystalline and well-oriented fiber and its polymers are weakly hydrogen bonded. Therefore, polyester fibers have high tenacity and are highly resilient. At low stress, they have high elastic recovery; at high stress, particularly repeated high stress, they have low elastic recovery. Polyester fiber is smooth and even in diameter and its cross-section is nearly circular. Its diameter varies from 12 to 25 μm, depending on end-use requirements.

Polyester products are available as filament fiber, staple and tow fiber, fibrefill, and non-woven structures. Polyester filament yarns, as well as spun yarns blended with cotton or rayon, are widely used in woven fabric and knitted fabric. These fabrics are attractive, durable, comfortable (except in conditions of high temperature and humidity), retain their appearance well, and are easy care.

Acrylic

Acrylic is a manufactured fiber in which the fiber-forming substance is any long-chain synthetic polymer composed of at least 85% by weight of acrylonitrile units. The first example was made in Germany in 1893. Since then, many efforts had been made to produce improved acrylic fibers. Du Pont started commercial production of the fiber in 1950, and was a major producer for the next 40 years. Acrylic is often available as staple fiber and tow. For apparel products use, its size varies from 1.2 to 3.0 denier. Acrylic fibers are usually slightly crimped, and their cross-section can be dog-bone shaped, kidney-bean shaped, or round.

Acrylic fibers are soft, warm, lightweight, and resilient. Because of their low specific gravity and high-bulk properties, acrylic fibers more successfully duplicate the positive aesthetic attribute of wool fibers. They are superior to wool in their easy-care properties and are non-allergenic. Acrylics are widely used in sweaters, socks, fleece fabrics and fake-fur fabrics.

Polyolefin

Polyolefin fibers are made from polymerized ethylene or propylene. They were originally developed for soled (plastics) applications. Since 1960, polyolefines fibers have been produced for use in textiles, as monofilament, multifilament, staple fiber and tow. They are rod-shaped and smooth-surfaced. However, their cross-section can be modified easily. Polyolefins are the lightest-weight fibers (SG < 1.0). Today, they are used for thermal underwear, socks, sweaters, and active sportswear.

10.1.4 New developments in textile fibers

Despite the long history and maturity of fiber science, new processes, materials and products are still being developed today. Many new fibers with unique characteristics for special use have been developed. Here, some of them are introduced.

Elastomeric fibers

An elastomer is a natural or synthetic polymer that, at room temperature, can be stretched repeatedly to at least twice its original length, and upon immediate release of the stretch, will return to approximately its original length. Spandex and rubber are two major elastomeric fibers used in apparel. Rubber fibers are manufactured fibers in which the fibre-forming substance is comprised of natural or synthetic rubber. Rubber is rarely used as a bare filament; it is generally the core in a covered yarn.

The first synthetic elastic fiber, a spandex fiber called 'Lycra™', was produced Du Pont in 1958 after many years of research. Spandex fibers are superior to rubber in strength and durability. They are produced as monofilament or multifilament yarns in a variety of deniers. Spandex is seldom used alone in fabrics. Other fibers or yarns are added to achieve the desired hand and appearance. Spandex is mostly used in foundation garments, active sportswear, dancewear, hosiery, and narrow fabrics. It also has medical uses, such as surgical and support hose, bandages and surgical wraps (see Chapter 9).

Micro-fibers

One of the most important developments in textiles fibers has been the technology to extrude extremely fine filaments while maintaining all of the strength, uniformity and processing characteristics expected by textile manufacturers and consumers. Micro-fiber is defined as a fiber of less than 1.0 denier, so it is even finer than luxury natural fibers such as silk. It can

be extruded by reducing the polymer output at the spinneret and drawing with a large draw ratio. There are primarily three methods for micro-fiber production: direct spinning, mechanical splitting and solvent splitting.

Micro-fibers are available in two types: continuous filament and random staple. Their designed characteristics are extreme softness, high flexibility and smoothness. Their lower bending rigidity, high surface area and greater number of fibers per unit weight enable the production of fabrics that are softer, quicker drying and have greater cover and cooler hand.

High-performance fibers

High-performance fibers are driven by special technical functions that require specific physical properties unique to these fibers. They usually have very high levels of at least one of the following properties: tensile strength, operating temperature, limiting oxygen index (fire retardancy) and chemical resistance. Here, fibers with high mechanical performance are focused on. Meta-aramids are the most widely used specialized fibers, for their combination of heat resistance and strength at reasonable cost. Nomex from the Du Pont company and TeijinConex from the Teijin company are the well known meta-aramid fibers. Para-aramid fibers have similar operating temperatures to meta-aramid fibers, but have 3–7 times higher strength and modulus. 'Kevlar' (DuPont), 'Twaron' (Akzo) and 'Technora' (Teijin) are typical para-aramid fibers. They are ideal for reinforcement and protective type applications and usually are used in parachutes, bullet-proof vests, ballistic protective fabric, and cut-resistant fabric.

Carbon fiber can vary in both modulus and strength in large ranges depending on the raw material used and final heat treatment temperature. It is mainly utilized in specialized composites for the aerospace and similar industries.

Smart fibers

Shape-memory materials are able to memorize a second, permanent shape besides their actual, temporary shape. After application of an external stimulus, for example an increase in temperature, such a material can be transferred into its memorized, permanent shape. The process of programming and restoring a shape can be repeated several times. Shape memory polymers have been applied to textiles in fiber, film and foam forms, resulting in a range of high-performance fabrics and garments, especially sea-going garments.

There are also some smart fibers that are capable of measuring internal strain, temperature, humidity and so on. They can be made and integrated into textile structures such as yarns, fabrics and composites.

10.2 Structure parameters and measurement

10.2.1 Fine structure

Fine structure is a depiction of the arrangement of the polymers and the bonds that hold them together. The ability of a fiber to withstand mechanical forces is largely determined by its fine structure. Orientation and crystallinity are two major parameters to describe the fine structure of a fiber. Absorption of infra-red radiation, optical and X-ray diffraction studies, electron microscopy, and nuclear magnetic resonance are common methods used to investigate the fine structure of a fiber.

10.2.2 Fiber dimensions

Conditioning and testing of textile fibers must be carried out under constant standard atmospheric conditions. The standard atmosphere for textile testing involves a temperature of 20 ± 2 °C and a relative humidity of 65 ± 2%.

Size

There are a number of different ways of measuring fiber size/diameter, which differ fundamentally in their definitions of size, so that the measurements may not be easily inter-coverted. The gravimetric method is based on the relationship that for a given fiber its mass is proportional to its cross-sectional area. The fiber linear density is measured by weighing a fiber of a certain length on a balance. If the fiber has a circular cross-section, its diameter can then be calculated from the linear density. The projection microscope test (BS 2043) is the standard method for measuring wool fiber diameter, and is also applicable to any other fibers with a circular cross-section. A microscope slide of short lengths of fiber is prepared, and is then viewed using a microscope that projects an image of the fibers onto a horizontal screen for the diameter measurement.

The airflow method is an indirect method of measuring fiber fineness based on the fact that the airflow at a given pressure difference through a uniformly distributed mass of fibers is determined by the total surface area of the fibers.[1–5] The surface area of a fiber is proportional to its diameter but, for a given weight of sample, the number of fibers increases with the fiber fineness so that the specific surface area (area per unit weight) is inversely proportional to fiber diameter.[6] The airflow measurement is often used for wool and cotton fibers. The Shirley fineness and maturity tester (FMT) is also a kind of airflow method for cotton fiber.

The optical fiber diameter analyzer (OFDA)[7] is a microscope-based system which effectively automates the projection microscope. The system was originally developed for wool testing but is also capable of measuring other animal and man-made fibers. The CSIRO fiber diameter analyzer (FDA) is a non-microscopical system of measuring fiber diameter that operates by light scattering.[8,9]

In general, the finer the natural fiber size, the higher the quality of the fiber. Manufactured fibers are available in a wide range of sizes. They are classified as coarse (>7 dtex), regular (2.4–7.0 dtex), fine (1.0–2.4 dtex), micro (0.3–1.0 dtex), and ultra-fine (<0.3 dtex).

Length

The length of natural fibers is not constant but has a range of values. However, man-made fibers can be cut during production to whatever length is required, either with all the fibers of the same length or with a distribution of lengths. In the case of fibers with a distribution of lengths, a mean length is taken. There are two main types of methods to measure fiber length: the direct measurement of single fiber mainly for research purposes and tuft methods that involve preparing a tuft or bundle of fibers arranged paralleled to one another. The Wira fiber length machine is designed for direct measurement. It is an attempt to automate the process of single fiber measurement and is intended mainly for measuring wool fiber.[10] The comb sorter,[11,12] clamped tuft method,[13] Fibrograph,[14] Wira fiber diagram machine, and Almeter[15] are all for the tuft measurement. The comb sorter is used for cotton and wool measurement. The clamped tuft method, the Wira fiber diagram machine and the Almeter are for wool fiber measurement while the Fibrograph is an automatic method of measuring the fiber length of a cotton sample. Some image-based methods have also been developed for fiber length measurement.[16] The Fiber Quality Analyzer (FQA)[17,18] is an image processing system for investigating various fiber properties including length.

A trend in fiber measurement is that several existing instruments for various fiber parameter tests are integrated into a set of instruments, or new types of instruments are developed for measures covering many parameters of the fibers. These sets are known as High-Volume Instruments (HVI). The Spinlab system is one such system, which measures seven parameters of cotton fiber: fiber length, length uniformity, strength, elongation, micronaire, color and trash.[19] The Uster AFIS (Advanced Fibre Information System) is another typical system for single fiber testing covering the assessment of fiber length, fineness, maturity distribution and other dimensional parameters.

Cross-section shape

The shape of a fiber's cross-section is important in many applications. It has a considerable influence on bending stiffness and torsional stiffness of the fiber. Consider the bending stiffness of the solid fibers; those with round cross-sections offer a high resistance to bending and, hence the fibers are stiff. However, fibers with ribbon-like cross-sections, such as cotton, offer the least resistance to bending. The cross-section shape is usually observed under a microscope. Natural fibers usually have characteristic cross-sections determined by nature. The cross-sections of most manufactured fibers can be modified easily.

10.3 Fiber mechanical properties

10.3.1 Testing

Tensile

The stress–strain curve of a fiber is usually obtained by gradually extending it and measuring the tension corresponding to each increase in length. Because of the way in which the elongation and the breaking point of textile fibers varies with time, the method of stretching the specimen is an important factor in determining the results of the test. There are two different ways of carrying out tensile tests with regard to the way of stretching the specimen:

(i) Constant rate of extension (CRE), in which the rate of increase of specimen length is uniform with time and the load measuring mechanism moves a negligible distance with increasing load. The Instron Tensile Tester operates in this way.
(ii) Constant rate of loading (CRL), in which the rate of increase of the load is uniform with time and the specimen is free to extend, the elongation being dependent on the extension characteristics of the specimen at any applied load. The Krais instrument,[20] and the Scott IP testers[21] provide this method.

Universal testers are available in which the principles of constant rate of loading or constant rate of elongation can be used, either of the two modes being selected. The Cambridge Textile Extensometer is of this type.

Properties in various directions

Bending: There are few instruments developed for the bending test of a fiber. However, several approaches to measure bending have been described

in reference 22. A tensile tester can be modified for the measurement of flexural rigidity of coarse fibers. A fiber can also be formed into a circular loop for measuring the bending rigidity by studying the deformation of the loop under an applied load. By measuring the deflexion of filaments of short lengths, clamped at one end and loaded at the other, the bending rigidity can also be obtained. Fiber bending can also be measured dynamically. In this case, a bending stress–strain curve is obtained. Chapman's fiber-bending tester is a successful instrument for such a test.[23,24] The KES-FB2 bending tester, which was developed for a fabric bending test, can also be used to obtain a bending stress–strain curve for fibers.[25]

Torsion and shearing: Morton and Permanyer developed an apparatus to measure the torque–twist relation of a fiber.[26,27] Owen used a double-pendulum method to test the dynamic twisting.[28] By using KES-twist testing, a torque–twist curve can also be produced. Thus, the torsional rigidity can be obtained. It is difficult to measure directly the relation between shear stress and shear strain. The shear modulus is often calculated from the torque–twist curve.

Compression: Axial compression and transverse compressive properties are important in modeling the mechanical behavior of fibers, especially high-strength and high-modulus fibers. The axial compression modulus is often regarded as the same as the tensile modulus. Direct study of axial compression has been made by cutting sections of fibers or monofils and compressing them between plates. The method can also be used to study the transverse properties. The KES-FB3 tester can be used to obtain a pressure–thickness curve of fiber transverse compression.[25]

Friction: Since it is difficult measure the friction of a fiber against another surface or the inter-fiber friction, there are few commercial instruments for friction measurement. However, researchers have designed many apparatuses to deal with this issue. Based on the geometry of the contact area, methods for assessing fiber friction can be divided into four groups: (i) friction between two individual fibers; (ii) friction between a single fiber and one or more fiber assemblies; (iii) friction between two fiber assemblies; and (iv) friction between a single fiber and another surface. In these tests, fiber-to-fiber friction can occur at point, line and area contacts. Figure 10.1 illustrates the three contact modes.

Howell developed many approaches in order to carry out a point contact test for fiber friction: Howell's Method,[29,30] Hanging Fiber Method,[31] Inclined Fiber Method,[32] and Capstan Method.[33] The Cantilever Method[34] is also a point contact method. For the line contact test, there are the Twist Friction Method,[35] Capstan Method,[36,37] and Fiber Pull-out Method.[38–41]

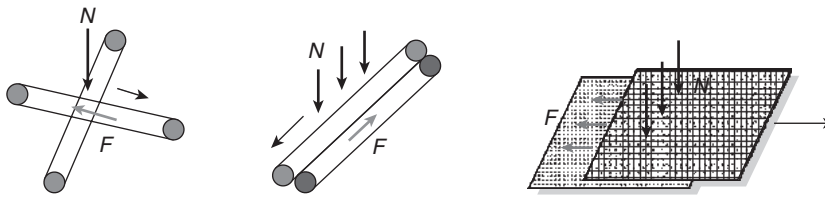

(a) Point contact (b) Line contact (c) Area contact

10.1 Contact modes of fiber friction.

Table 10.1 Fiber-on-fiber friction

Fiber pairs		Friction coefficient, μ	
		Static	Kinetic
Wool-on-wool[50]	with scales	0.13	0.11
	against scales	0.13	0.11
Rayon-on-rayon[51]		0.35	0.26
Nylon-on-nylon[51]		0.47	0.40

Due to anisotropy and viscoelasticity, the line contact and point contact methods may provide different kinds and amounts of contact and thus different frictional responses. Since the area contact method provides small variation in the inter-fiber friction, it may provide more representative and more reproducible results than other methods. There have been many methods and apparatus developed for measuring friction between assemblies.[42–48] It should be mentioned that, depending on the friction measuring device, the values of friction index responses will be different. Hong and Jayaramen have given a detailed review of the developments of fiber friction measurements in reference 49. Table 10.1 lists coefficients of fiber-on-fiber friction for several kinds of fibers.

10.3.2 Properties

The major mechanical properties of various common textile fibers are compared in Table 10.2.

10.4 Conclusion

In this chapter, the brief development history, structural features and mechanical properties of textile fibers have been introduced and the measurement of the relevant properties reviewed.

Table 10.2 Mechanical performance of various fibers

Fiber	Tenacity	Elongation	Initial modulus	Elastic recovery	Flexibility	Stiffness	Resilience	Toughness
Wool	Low	High	Low	High	High	Low	High	Low
Silk	Medium	Medium	Medium	Medium	–	Medium	Medium	High
Cotton	Medium	Low	Medium	Low	Low	Medium	Low	Low
Rayon	Medium	Medium	Low	Low	–	Low	Low	Medium
Acetate	Low	Medium	Low	–	–	Low	Low	Medium
Nylon	High	High	Low	High	High	Medium	High	High
Polyester	High	High	High	High	High	Medium	High	High
Polyolefin	High	Medium	Medium	High	–	Medium	Medium	High
Acrylic	Medium	Medium	High	Medium	–	Low	Medium	Medium

10.5 Acknowledgement

We would like to thank Hong Kong Polytechnic University for funding this research through Projects A188 and G-YD31.

10.6 References

1. BS 3183, *Method for the Determination of Wool Fiber Diameter by the Airflow Method*, British Standards Institution, London.
2. IWTO-28-29, *Detemination by the Airflow Method of the Mean Fibre Diameter of Core Samples of Raw Wool.*
3. BS 3181, *Part I: Determination of Micronaire Value by the Single Compression Airflow Method.*
4. ASTM D 1448, *Micronaire Reading of Cotton Fibers*.
5. Guse, P. *et al*., Optical Measurement of Fiber length in an Airstream. *Melliand Textilberichte/International Textile Reports*, 1995. **76**(3): p. 110–112.
6. Sommerville, P.J., Fundamental Principles of Fibre Fineness Measurement: The Airflow Instrument. *Wool Technology and Sheep Breeding*, 2000. **48**(2): p. 102–1046.
7. Baxter, B.P., Brims, M.A. and Taylor, T.B., Description and Performance of the Optical Fibre Diameter Analyser (OFDA). *Journal of the Textile Institute*, 1992. **83**(4): p. 526.
8. Irvine, P.A. and Lunney, H.W.M., Calibration of the CSIRO Fibre Fineness Distribution Analyser. *Textile Research Journal*, 1979. **49**: p. 97–101.
9. Lynch, L.J. and Michie, N.A., Instrument for the Rapid Automatic Measurement of Fibre Fineness Distribution. *Colourage*, 1981. **28**(14): p. 29–35.
10. BS 6176, *Method for Determination of Length and Length Distribution of Staple Fibres by Measurement of Single Fibres*.
11. BS 4044, *Methods for Determination of Fibre Length by Comb Sorter Diagram*.
12. ASTM D 1440, *Length and Length Distribution of Cotton Fibres (Array Method)*.
13. Anon, The Measurement of Wool Fibre Length. *Wool Science Review*, 1952. **9**: p. 15.
14. ASTM 1447, *Length and Length Uniformity of Cotton Fibres by Fibrograph*.
15. Schenek, A. and Janetzky, I., Almeter Test Method, a Possibility for Fiber Length Measurements on Raw Cotton. *Melliand Textilberichte/International Textile Reports*, 1990. **71**(12): p. 930–938.
16. Ikiz, Y. *et al*., Fiber Length Measurement by Image Processing. *Textile Research Journal*, 2001. **71**(10): p. 905–910.
17. Robertson, G. *et al*., Measurement of Fiber Length, Coarseness, and Shape with the Fiber Quality Analyzers. *TAPPI Journal*, 1999. **82**(10): p. 93–98.
18. Trepanier, R.J., Automatic Fiber Length and Shape Measurement by Image Analysis. *TAPPI Journal*, 1998. **81**(6): p. 152–154.
19. Giddens, B., Spinlab: High-Volume Fiber Testing Instruments. *Textile World*, 1984. **134**(4): p. 123–126.
20. Krais, P., *Journal of Textile Institute*, 1928. **19**: p. T32.
21. Raes, G., Fransen, T. and Verschraege, L., *Textile Research Journal*, 1968. **38**: p. 182.

22. Morton, W.E. and Hearle, J.W.S., Tensile Properties, in *Physical Properties of Textile Fibres*. 1993, The Textile Institute. p. 265–305.
23. Chapman, B.M., *Textile Research Journal*, 1971. **41**: p. 705.
24. Chapman, B.M., *Journal of the Textile Institute*, 1973. **64**: p. 312.
25. Kawabata, S., The Development of the Objective Measurement of Fabric Handle. in *Second Australia–Japan Symposium on Objective Evaluation of Fabric Quality, Mechanical Properties, and Performance.* 1982. Kyoto: Textile Machinery Society of Japan.
26. Morton, W.E. and Permanyer, F., *Journal of the Textile Institute*, 1947. **38**: p. T54.
27. Morton, W.E. and Permanyer, F., *Journal of the Textile Institute*, 1949. **40**: p. T371.
28. Owen, J.D., *Journal of the Textile Institute*, 1965. **56**: p. T329.
29. Howell, H.G., *Journal of the Textile Institute*, 1951. **42**: p. T521.
30. Mogahzy, Y.E.E. and Gupa, B.S., *Textile Research Journal*, 1993. **63**: p. 219.
31. Briscoe, B.J. and Motamedi, F., *Textile Research Journal*, 1990. **60**: p. 697.
32. Howell, H.G. and Mazur, J., *Journal of the Textile Institute*, 1953. **44**: p. T59.
33. Howell, H.G., *Journal of the Textile Institute*, 1953. **44**: p. T359.
34. Basu, S.C., Hazma, A.A. and Sikoski, J., *Journal of the Textile Institute*, 1978. **69**: p. 68.
35. Lindberg, J. and Gralen, N., *Textile Research Journal*, 1948. **18**: p. 287.
36. Roder, H.L., *Journal of the Textile Institute*, 1953. **44**: p. T247.
37. Schick, M.J., *Textile Research Journal*, 1973. **43**: p. 103.
38. Postle, L.J. and Ingham, J., *Journal of the Textile Institute*, 1952. **43**: p. 239.
39. Cox, D.R., *Journal of the Textile Institute*, 1952. **43**: p. T87.
40. Denby, E.F. and Andrews, M.W., *Textile Research Journal*, 1965. **35**: p. 913.
41. Peirce, F.T. and Lord, E., *Journal of the Textile Institute*, 1939. **30**: p. T173.
42. Morrow, J.A., *Journal of the Textile Institute*, 1931. **22**: p. 425.
43. Martindale, J.G., *Journal of the Textile Institute*, 1947. **38**: p. T151.
44. Lord, E., *Journal of the Textile Institute*, 1955. **46**: p. 41.
45. Viswanathan, A., *Journal of the Textile Institute*, 1966. **57**: p. T30.
46. Viswanathan, A., *Journal of the Textile Institute*, 1973. **54**: p. 553.
47. Koza, W.M., *Textile Research Journal*, 1975. **45**: p. 639.
48. Mogahzy, Y.E.E. and Broughton, R.M., *Textile Research Journal*, 1993. **63**: p. 465.
49. Hong, J. and Jayaraman, S., Friction in Textiles, in *Textile Progress*. 2003, The Textile Institute, Manchester.
50. Zurek, W. and Frydrych, I., *Textile Research Journal*, 1993. **63**: p. 322.
51. Olofsson, Bard Gralen, N., *Journal of the Textile Institute*, 1950. **43**: p. 467.

11
Yarns

K.F. CHOI
The Hong Kong Polytechnic University, China

11.1 Introduction

Yarn structure has a strong influence on the biomechanical properties of the fabric produced. It is very difficult to quantify yarn structure and no published literature can be found which gives an unambiguous definition for important yarn quality parameters. Theoretically speaking, the structure of a yarn can be quantified by knowing the spacial arrangement of all the fibers in the yarn. With the incorporation of the fiber mechanical and dimensional properties, the collective behavior of the yarn can then be determined by considering the effect of individual fibers and their interactions. The above work requires tremendous effort and the reward is not attractive enough. Instead of measuring all the fibers in a yarn, a random sample of fibers is taken and the path of those fibers is quantified. This is the famous tracer fiber technique, first introduced by Morton.[1] Another important yarn structural property is the distribution of fibers in the yarn. The highly non-linear mechanical properties are mainly due to the non-uniform distribution of fibers. This can be explained by the shortest path hypothesis.[2]

11.2 General view of today's yarns

Ring spinning is regarded as the conventional yarn production process which has more than 150 years of history and will continue to be the most versatile and important process in the near future until an alternative method has developed to such a stage that it can be replaced over the whole count range. Air jet spinning is taking ground in the fine yarn count region. Rotor spinning has secured its share in the low to medium count sector. Friction spinning is still struggling to get rid of poor yarn strength and low yarn abrasion resistant problems. Other spinning methods, such as wrap spinning by hollow spindle, seem to be quite static in terms of further development. The sole motivation of searching for alternative spinning methods

is to increase productivity, since ring spinning reached its upper limit long ago.

It is expensive to add one turn of twist in the rotor and ring system because it involves one complete revolution of the rotor or the traveler around the ring. The production speed is also limited by the excessive yarn tension arising from the centrifugal force. For friction and air jet spinning, a turn of twist is inserted by rotating the yarn itself; thus it is more energy saving. In addition, the yarn tension is relatively low since the yarn withdrawal force is not directly affected by the action of twist insertion.

Yarns produced by different spinning processes vary quite significantly in yarn properties. As a standard of yarn quality, ring spun yarn is generally used to assess the success of other new processes by quality comparison. The assessment of yarn quality is becoming more stringent. The all-round yarn characteristics are compared. They include the yarn strength, unevenness, abrasion resistance, hairiness, bending stiffness and hand. Those yarn properties will be explained in relation to yarn structure and the measuring methods will be described in the coming sections.

Due to the difference in yarn structure, rotor yarn cannot be compared directly with ring yarn of the same twist level. Rotor yarns require a higher machine twist than ring yarns in order to achieve similar tensile strength levels. Twist measurement of rotor yarn is not straightforward since the wrapper fibers on the yarn surface cannot be untwisted. The direct untwisting method is surely not applicable. The single untwist-retwist method demonstrates large discrepancies. The French type multiple untwist-retwist method has, however, been shown to give accurate measurement of machine twist.

New spinning systems differ from conventional ring spinning systems in regard to the yarn twisting mechanism; they produce yarns with different fiber configuration and packing density distribution. Fibers in ring yarn are well aligned and interlocked with a migratory geometry. In rotor yarn a bicomponent structure can be observed; a regularly twisted core covered by a sheath of entangled fibers which are occasionally wrapped by belt-like fiber.

The yarn-making process has two phases: phase I – Fiber feeding stage (drafting and transport), phase II – Yarn formation stage. Fiber cohesion is obtained by twisting, wrapping, entanglement, bonding or their combinations. (Fiber migration = twist + entanglement). A major drawback of break spinning is lack of sufficient fiber tension during the spinning process. Productivity of rotor yarn is limited by the pull-out tension (proportional to $r \cdot w$), but tension in spinning zone is still low.

In terms of production speed, ring spinning is left far behind to those new spinning methods such as rotor spinning, friction spinning and air jet spinning, and especially by the MVS air jet, where the production speed can

reach up to 400 meters per minute. This is about 20 to 30 times more productive than ring spinning. Nevertheless, ring spinning is still the most popular yarn production method, partially due to the technology inertia. Most people are reluctant to change when the existing system is running fine. Changing will mean further investment and uncertainty. Adopting new technology may cost quite a lot since new versions with certain improvements come out too often. Everyone wants to wait until the technology matures. Another major reason for the popularity of ring spinning is the quality of yarn produced. Ring spinning has its unique yarn formation mechanism such that all the fibers are subject to a certain level of tension. High-tension fibers tend to move toward the yarn center, low-tension fibers tend to buckle out toward the yarn surface. This periodic movement of fibers in a yarn causing a variation of radial position is called fiber migration. The moving in and buckling out mechanisms occur simultaneously, resulting in a self-locking structure. The self-locking structure of ring spun yarn contributes significantly to the high tensile strength and good abrasion resistance.

The self-locking mechanism is enhanced by moderating the fiber tension just before yarn formation. It is the basis of Solospun yarn. A Solo roller with intermittent grooves on the roller surface can enhance the degree of fiber migration such that fibers interlace to a larger extent. It is found that the yarn tensile strength is not further increased, but the abrasion resistance is improved remarkably.

11.3 Yarn structural properties

11.3.1 Fiber path in yarn

The fibers in a ring spun yarn in general follow helical paths with varying helix radii. This is the well known phenomenon called fiber migration. As described by Morton,[1] the spinning tension acting on individual fibers causes the fibers to move away or toward the yarn axis. The migration pattern of ring yarn is very different from other yarn types. For example, open end friction spun yarn (produced using the DREF 2 system) is found[3] to have stronger migration than ring yarn, but the migration is unidirectional, i.e. one end of fiber lies on the yarn surface and the other end in the yarn core. The fibers form conical helices with much intermingling (interlacing), to form a well-locked yarn structure. The fiber migration of friction spun yarn is facilitated by geometrical means instead of mechanical means as for the ring spun yarn. During the yarn forming process, fibers, after passing through the opening roller, are laid on the surface of a conical yarn tail which is rotating on the nip of the suction roller. The so-called 'length utilization' of fiber in friction spun yarn is poor. Quite a number of fibers

wrap loosely around the yarn surface. Tracer fiber technique is an effective way to study the fiber path in a yarn. Together with the image analysis algorithm, a large number of tracer fibers can be sampled and a better representation of the yarn structure can be obtained. The yarn cross-section analysis provides some further information on the yarn structure, for example the fiber packing density distribution[4] in a yarn. It is a very important yarn parameter which is related to the highly non-linear torsional and tensile properties of yarn,[5] and the initial lateral compression modulus of fabric and hence fabric handle.

11.3.2 Packing density distribution of yarn

Some other very interesting results concerning yarn structure can be obtained from yarn cross-section analysis, for example (i) the hollow center[6] of yarn due to ribbon twisting in worsted spinning, (ii) fewer fibers in a cross-section of rotor yarn than that of ring yarn of the same count and twist due to poor alignment of fibers in the rotor yarn, (iii) friction yarn has a loose packing[7] of fibers in the yarn cross-section due to low tension present during yarn formation, and so on.

The packing density distribution has a significant effect on yarn mechanical properties, especially the initial tensile modulus. According to the shortest path principle,[2] fibers will move toward the yarn center to avoid being strained until the yarn core is jammed (i.e. packing density has reached the upper limit). When the yarn is quite loose in the core region initially, it will have room for yarn extension before the yarn core becomes jammed with fibers and forces most of the fibers to extend. The work done to extend the fibers is much larger than that for bending and twisting the fibers. Moving the fibers toward the yarn center only involves bending and twisting fibers. With the same amount of yarn extension, the larger work undertaken means a larger yarn modulus. Methods of measuring fiber packing density are described in the following sections.

Conventional method

The conventional method[4,8] of fiber lateral distribution measurement is called the slice cutting method. The procedures of this method involve fixing the yarn by means of resin and cutting thin slices of the yarn. The fibers in the yarn cross-section can then be analyzed manually or automatically by means of image analysis. In the experiment, the yarn length is under control such that the yarn cannot contract when immersed in the resin. The cross-section of the yarn in an extended or twisted state can also be studied using this method. It is a very useful tool for the analysis of fiber movement in a yarn when subject to external forces.

When a yarn is being deformed, it could be quite compact, so the viscosity of the resin fixing agent should be low enough to penetrate into the spaces between fibers in the yarn. In addition, the fixation process of the fixing agent should take place even though it is at room temperature. Based on the above requirements, an acrylic resin with its catalyst was selected. With suitable proportions of resin and catalyst giving the right amount of setting time, very satisfactory thin slices of the yarn cross-sections can be obtained by use of a microtome.

When a yarn is immersed in a liquid, there will be a change in fiber arrangement. Generally the yarn will increase in diameter but decrease in length. One way to minimize the change in fiber arrangement is by controlling the yarn length. A clamp was specially designed for this purpose. The yarn was threaded through a plastic tube, and then the yarn and the plastic tube were fixed together on the clamp, with the lower jaw closed firmly such that resin would not leak through. By inverting the clamp, the yarn was tensioned under its own weight. The clamp was restored to its upright position after the upper jaw was firmly closed. The resin was mixed with the catalyst according to the proportions stated in manufacturer's manual. The newly prepared resin was injected into the tube as soon as possible. The resin was allowed to set and cool in air for about one hour. The yarn in the resin was then removed from the tube and thin slices were cut using a standard microtome with a steel knife.

The slices were viewed under the microscope and the images were captured. By enlarging the photograph to a scale of 200:1, each fiber cross-section was represented by two quantities: coordinates of the center of mass and area of cross-section. To calculate the mass of fiber at different yarn radial positions, annuli with equal areas were constructed. The area of fiber cross-section at each annulus was determined by representing the fiber cross-sections by circles with same area and center of mass. A computer program was used to perform the calculation and produce the lateral yarn density function.

The disadvantages of the slice cutting method are that, first, the yarn structure may be changed in the resin bath, and secondly this method is a destructive test; as a result the same portion of yarn cannot be used for other tests. In addition, the method is tedious and time consuming to carry out.

Measuring method using computed tomography principle

In this section a novel method of measuring the yarn density distribution is introduced. A technique based on the principle of computed tomography[9,10] (CT, e.g. human body scanning) is introduced. According to a literature search, the principle of CT has never been applied in the textile field

before. The selection of the penetrating source is the most important part in the construction of the measuring device. The penetration power of the source is acceptable when it can penetrate most of the commercial yarn. The sensitivity of the detector is acceptable when the absorption of a single fiber can be detected. The reliability of the new measuring device will be justified by means of the conventional yarn cross-sectional analyzing method which was described in the previous section.

The proposed method could eliminate the shortcomings of the conventional method, which are that, firstly, the yarn structure might be changed by immersion in the resin, and secondly that it is a destructive test. With an automated system for the measurement of yarn structure, any new yarn structures achieved by modifying the spinning methods or spinning conditions may be quantified quickly. This will further assist in future investigations related to yarn mechanics. In addition, the new measuring device could be attached to a spinning machine to provide on-line monitoring of the yarn quality. Since even the packing density distribution of yarn can be measured, all the yarn faults and levels of irregularity can also be measured with ease.

The experimental set-up is shown in Fig. 11.1. An X-ray diffractometer was used for the scanning experiment. The copper target of the X-ray tube was energized at 30 keV, the tube current was limited to 20 mA. A circular, stainless-steel tube and an aperture were used to collimate the X-ray beam to a size of about $2 \times 5\,\text{mm}^2$.

As yarn is produced by twisting fiber strands, it is reasonable to assume the packing density of yarn is axially symmetric. With this assumption, the absorption profile in one direction is enough to reconstruct the cross-section image of the yarn. Obviously, taking the average along the yarn length would get a more representative packing density distribution of the yarn.

The yarn was mounted on a linear positioning stage that was equipped with a digital micrometer of 1 μm reading resolution. It was exposed to the

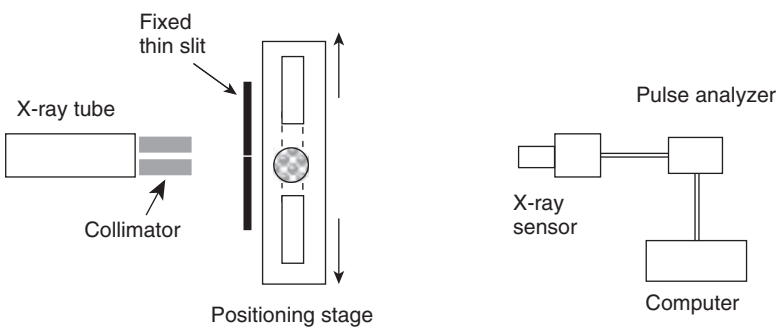

11.1 Schematic diagram for the X-ray scanning experiment.

collimated X-ray radiation at the rear of a 0.1 mm slit. A focusing optic system including a 0.1 mm aperture slit, and a 1/2° field of view slit were used for the X-ray collection. A solid state detector received the X-ray radiation and the signal was fed through a pulse height analyzer and then recorded by a microcomputer. In order to deduct the background, the X-ray intensity was measured by scanning the detector for a small angle in each measurement.

Experimental result: Two woolen carpet yarns were produced at Canesis Network Ltd. (former WRONZ); one was high twist, the other low twist (see Fig 11.2). The specifications of the yarns are given in Table 11.1. The relative X-ray absorption curves of the yarns are shown in Fig. 11.3. The high-twist yarn has a higher degree of absorption at the yarn core region. The absorption region of the low-twist yarn spreads over a relatively larger distance. Another obvious difference of the two yarns is related to the symmetry of the absorption curves. High-twist yarn has a more symmetric absorption curve. It is as expected since twisting a fiber strand would make it more axial symmetric.

Principle of computed tomography: Transmission CT is applied here. A cross-section of the yarn is scanned by a thin X-ray beam whose intensity

Table 11.1 Parameters of yarns

Yarn parameters	Low-twist yarn	High-twist yarn
Linear density (tex)	256	288
Twist level (turns per meter)	115	265
Yarn diameter (mm)	1.16	0.96

(a) Low-twist yarn (b) High-twist yarn

11.2 Cross-section of yarn.

loss is recorded by a detector and processed by computer to produce a two-dimensional image which is then used for the computation of the yarn density distribution.

The physical model of CT is as follows. Let $f(x)$ be the X-ray attenuation function of the yarn at location x. The X-ray traversing a small distance dx at x suffers the relative intensity loss dI/I, with $\mathrm{d}I/I = f(x) \cdot \mathrm{d}x$. Let I_o be the initial intensity of an X-ray beam L which is a straight line, and let I_1 be its intensity after having passed the yarn.

It follows that

$$\frac{I_1}{I_o} = \mathrm{e}^{-\int_L f(x) \cdot \mathrm{d}x} \qquad [1]$$

The scanning process provides the line integral of the function f along each of the lines L. From all these integrals the function f has to be restructured. The transform which maps a function on R^2 into the set of its line integrals is called the two-dimensional Radon transform. Thus, the reconstruction problem of CT is just the inversion of the Radon transform in R^2. In practice the integrals can be obtained only for a finite number of lines L. In a parallel scanning geometry a set of equally spaced parallel lines is taken for a number of equally distributed directions. It requires a single source and a single detector which move in parallel and rotate during the scanning process. The real problem in CT is to reconstruct f from a finite number of its line integrals, and the reconstruction procedure has to be adapted to the scanning geometry.

Special case: yarn with axial symmetric packing density distribution: When the packing density $\varphi(r)$ is axial symmetric, its determination becomes much simpler. In mathematical terms, the packing density function can be found by solving the following integral equation, with given absorption function $m(x)$, and the unknown function $\varphi(r)$,

$$\int_x^1 \frac{r\varphi(r)}{\sqrt{r^2 - x^2}} \mathrm{d}r = m(x) \quad \text{where} \quad 0 < r < 1, 0 < x < r \qquad [2]$$

The absorption curves as shown in Figure 11.3 were substituted into Equation (2). The packing density functions of the two yarns were determined as shown in Figure 11.4.

The new method provides a convenient way to measure the packing density distribution of yarn. In the preliminary experimental study, the packing density distributions of woolen yarn with two twist levels were measured. When observing the X-ray absorption curve in Figure 11.3 and referring to the corresponding yarn cross-section view in Figure 11.2, the choice of the X-ray source and the conditioning of the X-ray beam were proven to be very appropriate, and the measurement of yarn packing density distribution based on computed tomography is highly feasible.

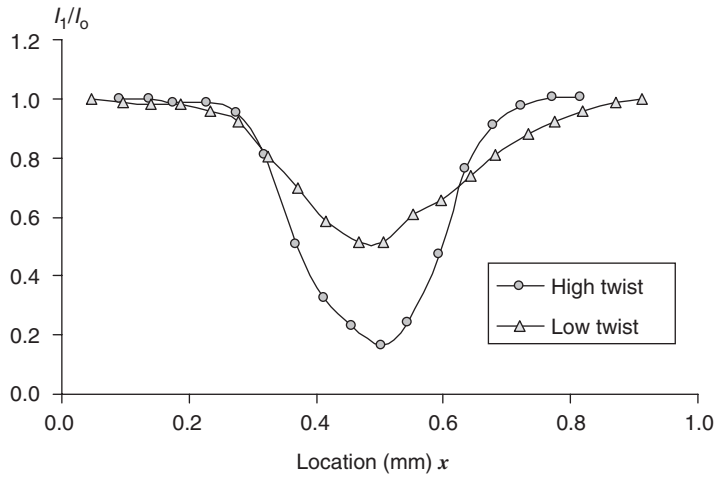

11.3 Relative X-ray absorption of yarns at different yarn locations.

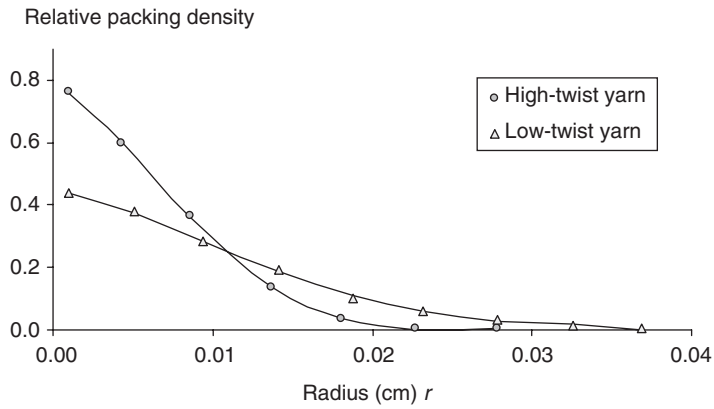

11.4 Packing density distribution of yarns.

11.3.3 Fiber interlacing

Fiber interlacing is the mutual consideration of fiber migration. If nearby fibers migrate in a similar pattern to the way that friction yarn's fibers migrate from core to surface due to the conical wrapping of fibers at the yarn tail during yarn formation, then fibers do not interlace much.

Some new yarn types, such as the Solospun yarns,[11] have proven successful in increasing the abrasion resistance, but the structure of the yarns could hardly be quantified in relation to the eminent properties using conventional method.[12–16] A new yarn structural parameter, average segment length

of fiber on the yarn surface, is proposed and described in this section. An initial experimental trial was performed for the purpose of verifying the usefulness of the new parameter in explaining the variation of abrasion resistance of yarns with different structures. Six types of worsted yarns were produced with varying degrees of fiber migration.

Surface length

A new measurement was introduced to quantify the degree of migration of fibers in yarn. It is the segment length of the fiber on the yarn surface (in short the 'surface length'). A particular fiber coming out of the yarn surface, staying on the yarn surface, and then re-entering into the yarn core would involve two random processes and the length of the fiber segment on the yarn surface would be affected by the surrounding fibers.

Dyed tracer wool fibers have been blended with other wool fibers in the spinning process. They could be observed when they come to the yarn surface. The distribution of segment length of the tracer fibers on the yarn surface reflects the fiber migratory behavior in the yarn. When a fiber undergoes a more idealized migration, it moves from the surface to the core and *vice versa*. If the fibers migrate more frequently, each fiber appears only momentarily on each superimposed concentric layer. Thus, it was postulated that the shorter the fiber exposing on the surface, the more the extent of migration. Consequently, the fibers are more likely to interlock with one another to provide a strong cohesion. It was expected that the shorter the surface length, the more frequent the fiber migration.

Surface length distribution

A segment of tracer fiber is seen on the surface of the yarn. With the aid of mirrors, the starting and ending points of the fiber segment can be located and then the surface length measured. By measuring the length of 100 surface segments of each yarn type, the cumulative distribution of the surface length of yarn type Y1 is plotted as shown in Fig. 11.5a. For the other yarn types, similar results can be obtained as shown in Fig. 11.5b–f. It was discovered that Gamma distribution functions $G(x)$ fit the cumulative distribution of surface length very well. Gaussian distribution functions (cumulative normal distribution) were plotted in Fig. 11.5 as well, for comparison purpose.

The following describes the principle of obtaining the Gamma distribution functions of surface length from the raw data. The generalized Gamma distribution is a three parameters (α, β and γ) distribution. The probability density function (pdf) of Gamma distribution $g(x)$ is the first derivative of the Gamma distribution function $G(x)$ and $g(x)$ is given by:[17]

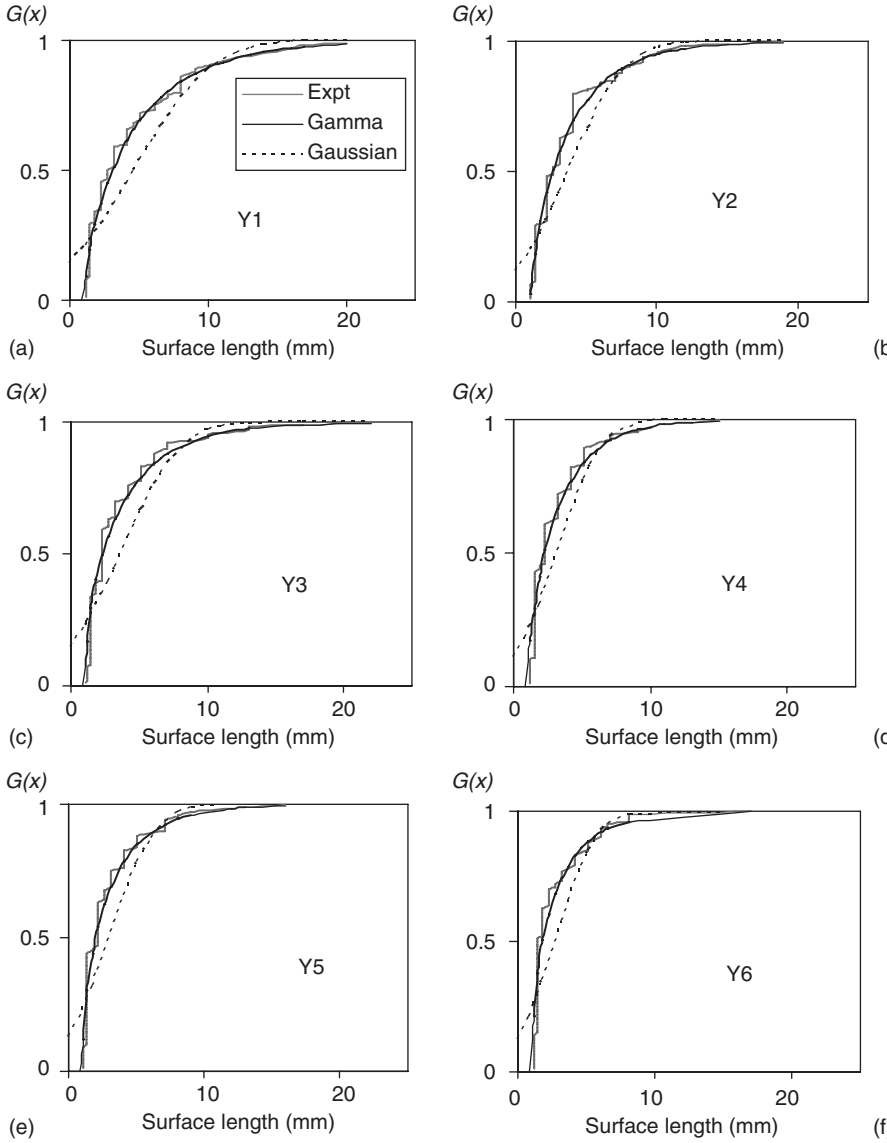

11.5 Distribution functions of surface length.

$$g(x) = \frac{1}{\Gamma(\alpha) \cdot \beta^{\alpha}} \cdot (x - \gamma)^{\alpha - 1} \cdot \mathrm{e}^{-\frac{x-\gamma}{\beta}}$$

where $\Gamma(\alpha) = \int_0^{\infty} y^{\alpha-1} \cdot \mathrm{e}^{-y} \cdot \mathrm{d}y$ and $x > \gamma$.

The mean of the distribution $\mu = \alpha\beta + \gamma$ and the variance $\sigma^2 = \alpha\beta^2$.

From the experimental data of surface length, the minimum surface length was found to be close to but not less than 1 mm. The estimate of the parameter γ was set to that value. The estimates of the remaining two parameters, α and β, could be calculated from the mean and variance of the surface length of the yarn. The means and variances of surface length of the six types of yarns and also the corresponding parameters' values are shown in Table 11.2.

With the values of the parameters given, the pdf for the yarns can be plotted as shown in Fig. 11.6. It was found that yarn type Y6 had the highest proportion of short surface length while yarn type Y1 had the least proportion of short surface length. For the sake of easy visualization, only yarn types Y1 and Y6 were plotted in Fig. 11.6.

Table 11.2 Summaries of surface length distribution for the six types of yarns

Surface length	Yarn type					
	Y1	Y2	Y3	Y4	Y5	Y6
mean (mm)	4.64	3.71	3.58	3.14	3.00	2.69
sd (mm)	4.43	3.17	3.46	2.58	2.67	2.35
Parameters						
α	0.67	0.73	0.56	0.69	0.56	0.52
β	5.40	3.71	4.64	3.12	3.55	3.28
γ	1.00	1.00	1.00	1.00	1.00	1.00

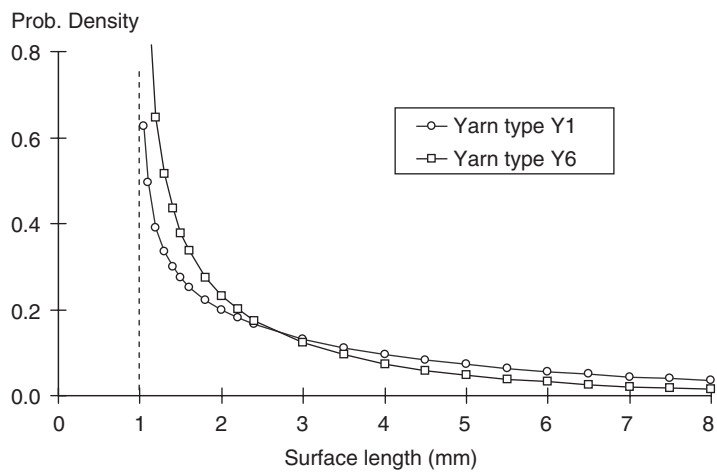

11.6 The surface fiber distribution of the yarns.

11.3.4 Twist and its measurement

Twist affects the yarn structure very significantly; in addition to the geometrical change, the change in fiber tension will affect the packing of yarn and the imposed torsional stress will affect the mechanical stability of the yarn. For a high-twist yarn, when the tension exerted on the yarn is not large enough, the yarn will buckle to become a tortuous shape. Due to the yarn formation mechanism, most yarn will have a large variation of twist at different radial positions, except ring yarn, so that only ring yarn can be untwisted to form a parallel fiber strand. This is the principle of twist measurement using the direct method.

A method based on different principles must be used for the twist measurement of other yarn types (e.g. rotor, friction and air jet). A method such as untwist-retwist, which is based on the twist contraction principle, could be employed, or its refinement; French type untwist-retwist, is a more satisfactory method.[18]

11.4 Yarn mechanics

11.4.1 Tensile properties

The mechanical behavior of yarns affects their suitability in most end uses. The most important yarn mechanical property is the tensile property. The strength of yarn is a crucial yarn specification. When the minimum yarn strength cannot be met, very poor production efficiency in the subsequent processes and inferior product quality will result. The factors affecting yarn tensile strength include yarn structure, fiber strength and fiber surface properties. Yarn mechanics in general refers to the yarn tensile, bending, torsional and abrasion properties. The mechanical properties of yarn include tensile tenacity, extensibility, elastic recovery, tensile modulus, bending stiffness, residual torque, and abrasion resistance under periodic tensile loading. For the measurement of yarn tensile properties a constant rate of extension meter is used – record load extension curve, extend, hold for a period, and release.

The yarn tensile test is well established. Standard testing methods are very popular in the textile field, e.g. the ASTM D2256 Standard Test Method for Tensile Properties of Yarns by the Single-strand Method. This test method describes the determination of tensile properties of monofilament, multifilament, and spun yarns, either single, plied, or cabled with the exception of stretch yarns. This test method covers the measurement of breaking force and elongation of yarns and includes ways of calculating breaking tenacity, initial modulus, chord modulus, and breaking toughness. Conditions of test are included for the testing of specimens that are: (i) conditioned in air, (ii) wet, not immersed, (iii) wet, immersed, (iv) oven-dried, (v) exposed

to elevated temperature, or (vi) exposed to low temperature. In the textile trade, the ultimate tensile strength, or breaking strength is taken into consideration. A yarn technologist would decide on the spinning method and the spinning parameters in order to produce yarns meeting the product specifications with optimum productivity.

The curve of total tensile strength of fibers is the upper bound of the tensile curve of staple yarn (see Figs. 11.7 and 11.8). The tensile load of a

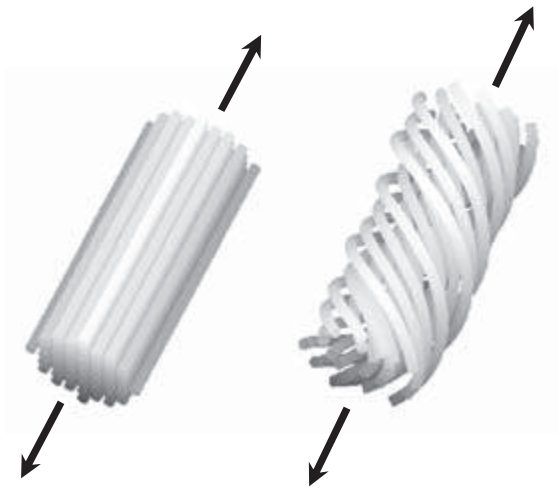

11.7 Fiber strands under tension.

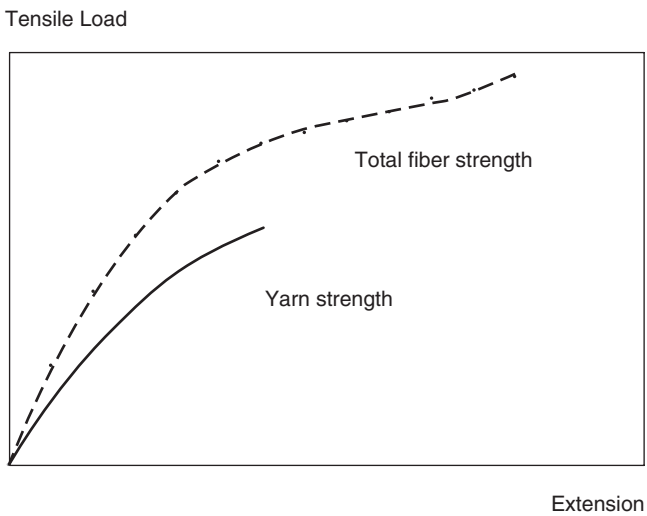

11.8 Load–extension curve.

yarn is always lower than the correspondent total fiber load. The reduction in tensile load is due to a mixture of the following reasons: Fiber slippage, fiber obliquity, loose packing of fiber, weak link effect.[19] Fiber slippage is inevitable for staple yarn; each fiber cumulates tensile stress at both ends from zero up to a stress level which is enough to extend the fiber with the same amount of extension of the yarn. Fiber tension contributes to yarn loading by a fraction of T_f only, which is $T_{//} = T_f \cdot \cos\alpha$, where α is the twist angle (helix angle) of the fiber. At higher twist levels, inter-fiber stress will increase and yarn failure due to excessive fiber slippage can be minimized. At the same time, fibers are more inclined to the yarn axis (with larger twist angle). Fiber load contributes less to yarn tensile load. The loose packing of yarn leads to an extra amount of yarn extension before tightening the fibers to bear the loading. Fibers in the outer yarn region will be straightened in a later stage. When the yarn is being extended, fibers tend to move toward the yarn center to avoid being strained until the yarn core is jammed, i.e. with close packing yarn density. The tensile strain distribution of fibers in a yarn can be calculated at various yarn extension states under the assumption that fibers are simple helices with equal helical pitch.

Even when the fiber is perfectly uniform and the spinning process does not introduce additional variation, the spun yarn will have inherent irregularity. The number of fibers in a cross-section follows a Poisson distribution. Within a length of yarn, there exists a minimum strength point at which the yarn breaks. This is the well-known weak link effect.[19]

11.4.2 Yarn torsional properties

Evaluation of yarn torsional properties is much less popular than that of yarn tensile properties since they are more difficult to measure and their effects are less readily related to the properties of final garment. Normally, people deal with these properties qualitatively. They use words such as twist lively yarn to refer to yarn with a high value of residual torque.

Yarn torsion meter

The most direct way to determine the torsional properties of a yarn is to measure the torque rotation relationship of the yarn with a torsion meter. The torsion meter (KES-YN1) used in this experiment was manufactured by the Kato Tech. Co. Ltd., Japan. The load range is from –500 mgf.cm to +500 mgf.cm. During testing, the yarn specimen is subjected to a constant tension and its length is allowed to change freely. The torsion meter is based on the torsion balance principle: a standard metal wire of known torsional stiffness is connected to the yarn at the upper end and the rotational displacement of the wire is measured by a very sensitive displacement

transducer. The amplified signals of the transducer output are sent to the plotter and a torsion rotation curve is obtained.

Singles yarn torsional properties

Singles yarn torque was measured using the KES-YN1 Yarn Torsion Meter. The twisting head in the instrument twisted the yarn specimen in a cyclic manner. The yarn tension was kept constant at 25 gf.

Specification of low-twist and high-twist yarns

Yarn type	: Woolen spun carpet yarn
Yarn linear density	: 256; 288 tex
Yarn twist level	: 115; 265 turns per metre (Z-direction)
Yarn state	: Boil-set (almost zero residual torque)
Yarn test length	: 3 cm
Fiber type	: New Zealand Romney Wool
Mean fiber radius	: 1.805×10^{-3} cm

The woolen yarns and the yarn specifications were supplied by Canesis Network Ltd (WRONZ) – see Fig. 11.9.

The mid-points of the yarn torque of the upper and lower hysteresis curves at different levels of yarn rotation were plotted in Fig. 11.10. The high-twist yarn has a larger torsional rigidity than the low-twist yarn and the torsional curve of the former is less linear. The low torsional rigidity of the low-twist yarn can be explained by its loose structure. Fibers can freely move to accommodate the overall twisting strain of the yarn before they form a compact yarn core to act against the imposed yarn torque.

11.4.3 Yarn bending properties

Yarn bending rigidity has a strong influence on fabric hand and appearance. The bending properties of yarns differ significantly from those of solid beams. They are strongly influenced by the restraint with which the fibers

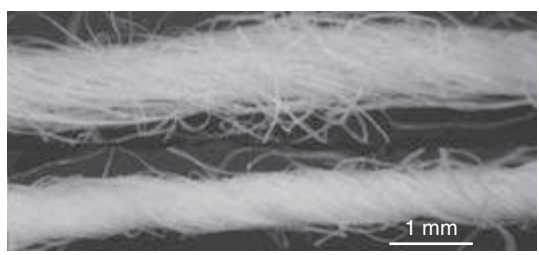

11.9 Longitudinal view of low- and high-twist yarns.

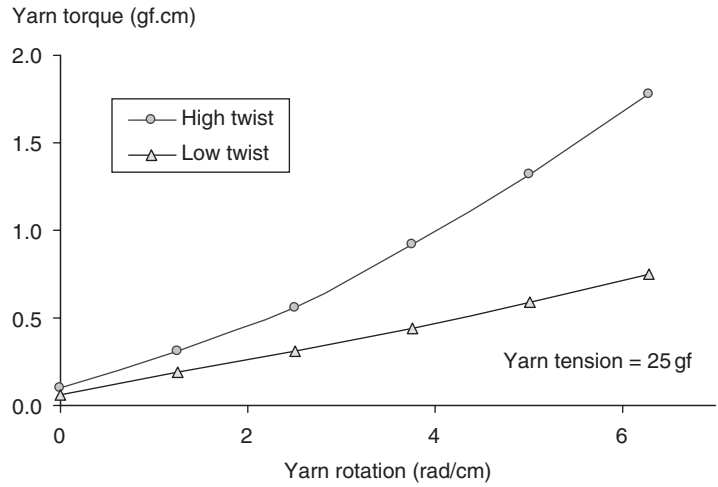

11.10 Torsional properties of yarns with different twist levels.

can move relative to each other in order to accommodate local deformations due to bending. The degree of the constraint is governed by the twist level of the yarn and the surface properties of the fibers. For loose yarns, the fibers can be assumed to bend independently with each other. In this case, the yarn-bending rigidity is effectively equal to the sum of the bending rigidities of individual fibers. Thus, the bending rigidity of such a yarn is proportional to the number of fibers in its cross-section.

In his theoretical study of yarn bending, Backer[20] calculated the local fiber strains for two extreme cases of deformation: complete freedom of relative fiber movement and no relative fiber movement. It was postulated that when the fibers were completely free to change their paths in the yarn, no fiber strain would be developed during yarn bending, and that when complete restriction of fiber movement was imposed, maximum strains would occur in the fibers lying on the outside (with tensile strain) and inside (with compressive strain) of the yarn torus. For real yarns, the mobility of fibers must lie in-between the two extreme cases, and should be closer to the complete freedom case.

Although the Bending Tester is designed to measure fabric bending rigidity, it can also be used to measure the bending properties of yarn. During testing, a number of yarn samples are laid parallel with equal spacing and under uniform tension. Then both ends of the samples were secured using double-side adhesive tapes and paper strips. During testing, the yarns were allowed to bend freely between two clamps spaced 1 cm apart. Bending hysteresis curves were obtained from the KES-FB2. The

bending rigidity and coercive bending moment of the yarns can also be measured.

Specification of yarn

Yarn type	: Woolen spun carpet yarn
Linear density	: 256 tex
Yarn twist level	: 191 turns per metre (Z-direction)
Yarn radius	: 0.05 cm
Yarn state	: Boil-set (almost zero residual torque)
Fiber type	: New Zealand Romney Wool
Mean fiber radius	: 1.805×10^{-3} cm

A total of 64 yarns were laid parallel to one another during the test. The bending hysteresis curve was plotted as shown in Fig. 11.11. The bending curve was unexpectedly linear. This may be due to the fact that the bending deformation was very small since the maximum curvature of the yarn was just equal to 2 cm^{-1}. Comparing with the yarn diameter of 0.1 cm, the curvature should reach 10 cm^{-1}, which is the typical bending deformation of yarn in a knitted fabric. This is a limitation of using the KES-FB2 Tester for the measurement of yarn bending.

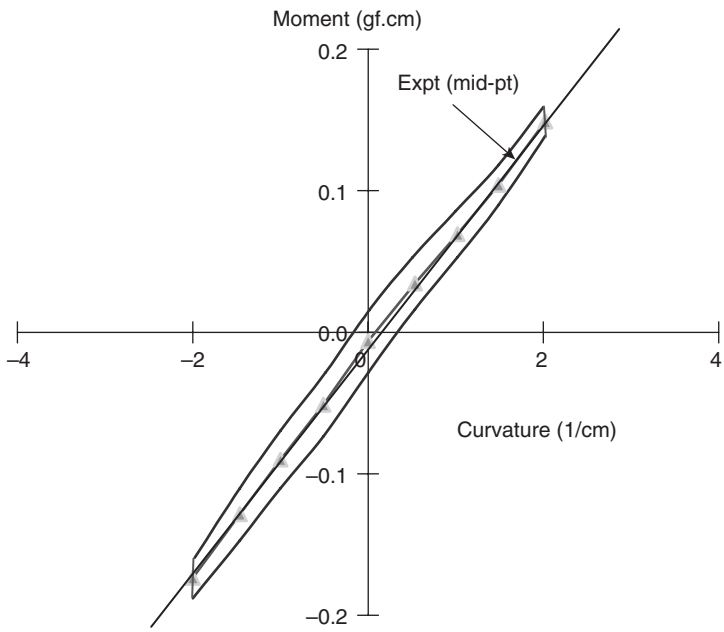

11.11 Bending properties of yarn.

11.5 Degree of fiber interlacing and abrasion resistance

Semi-worsted yarns of 46 tex and 600 turns per meter were processed in Canesis Network Ltd. (WRONZ). The processing parameters were varied such as to obtain a series of yarns with changing abrasion resistance.

Test on yarn abrasion resistance

Brorens *et al.*[21] evaluated the yarn abrasion-resistant properties at WRONZ using their specially designed abrasion tester. Unlike the normal 'rubbing' on the yarn surface, this tester performs the mechanism of yarn failure which is primarily a gradual drafting of the abraded area under abrasion.

In the experiment of yarn abrasion described in this section, the Shirley Yarn Abrasion Tester was used. The tester consists of two reciprocating bars: one is made of hardened steel and the other is covered with the standard abradant used in the Martindale Fabric Abrasion Tester. Eight yarn specimens were tested simultaneously. Yarns were threaded from the fixed holders and clipped onto the flexible holders on which sensors were attached. The initial tension exerted on each yarn was 0.5 N. When a yarn was broken, the flexible holder fell, a signal would be sent to the control unit, and the number of rubs for that particular yarn would be recorded.

The abrasion cycles were set to an upper limit of 10 000 rubs and the elongation of each yarn during test was recorded every 500 cycles. Twenty specimens were taken randomly from each yarn type for the test and the results were summarized in Fig. 11.12. It can be observed that yarns of type Y6 have the highest proportion of yarn specimens lasting for most abrasion cycles before breakage (with extension of more than 12%).

It was found that that yarn abrasion resistance was inversely proportional to the average surface length, and the coefficient of determination R^2 = 0.9481, i.e. around 94.8% of the variation of yarn abrasion resistance can be explained by the variable average surface length. As a result, a simple yarn structural parameter that is closely related to the yarn abrasion resistance properties was discovered. The merits of this new parameter include easy measurement and true reflection of the degree of interlacing of the fibers near the yarn surface. As the surface fibers are to be measured, there is no need to search for a suitable solvent to optically dissolve the fibers in the yarn such as to highlight the tracer fiber for measurement of spatial coordinates. This would save a lot of effort during preparation work and data processing for the generation of migration parameters.[12] In addition, the surface fiber length measurement has eliminated the error of varying yarn diameter which influences the location of the yarn axis and thus the accuracy of the migration parameters. More extensive experimental work

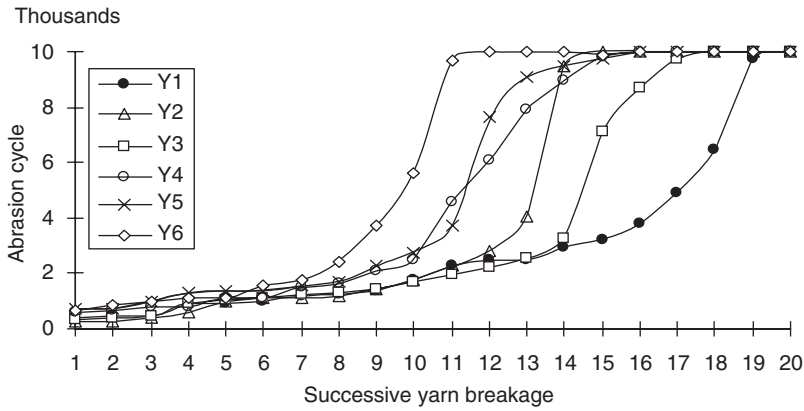

11.12 Abrasion resistance of the yarns.

will be performed to verify the reliability of the new structural parameter for different yarn types, e.g. Solospun.

11.6 Conclusion

In this chapter, a brief development history of yarns has been given, followed by a description of recent studies[22,23] on the most important yarn structural parameters, i.e. surface length distribution and lateral yarn density distribution. The major mechanical properties were briefly described. They include the tensile, bending, torsional and abrasion properties of yarns. The emphasis here is on studies of the inter-relationship between the yarn structure and mechanical properties. For details of the respective yarn properties, many papers can be found in the *Journal of the Textile Institute* and in the *Textile Research Journal*.

11.7 References

1. Morton, W.E., The Arrangement of Fibers in Single Yarns, *TRJ* 1956, **26**, p. 325–331.
2. Carnaby, G.A., The Structure and Mechanical Properties of Wool Carpet Yarns, *PhD Thesis* (University of Leeds), 1976.
3. Lunenschloss, J. and Brockmanns, K.J, Cotton Processing by New Spinning Technologies, Possibilities and Limits, *Int Textile Bull*, Yarn Forming 1986, (2) p. 7–22.
4. Hickie, T.S. and Chaikin, M., The Packing Density in the Cross-section of Some Worsted Yarn, *Journal of the Textile Institute*, 1973, **65**, 433–437.
5. Tandon, S.K., Carnaby, G.A., Kim, S.J. and Choi, K.F., The Torsional Behaviour of Singles Yarns – Part I: Theory, *Journal of the Textile Institute*, 1995, 185–199.

6. Hickie, T.S. and Chaikin, M., *Journal of the Textile Institute*, 1960, **51**, T1120.
7. Alagha, M.J., Oxenham, W. and Iype, C., Influence of Production Speed on the Tenacity and Structure of Friction Spun Yarns, *Textile Research Journal*, 1994, **64**, 185–189.
8. Neckar, B., Ishtiaque, S.M. and Svehlova, L., Rotor Yarn Structure by Cross-section Microtomy, *Textile Research Journal*, 1988, **58**, p. 625–632.
9. Natterer, F., *The Mathematics of Computerized Tomography*, Wiley, 1986.
10. Tasto, M., Reconstruction of Random Objects from Noisy Projections, *Computer Graphics and Image Processing*, **6**, p. 103–122.
11. Lappage, J., Weavable Singles Yarn Potential, *Wool Record* 1999, **158**, (3656) June p. 89.
12. Hearle, J.W.S., Gupta, B.S. and Merchant, V.B., Migration of Fiber in Yarns Part I: Characterization and Idealization of Migration Behavior, *Textile Res. J.* 1965, **35**, p. 329–334.
13. Hickie, T.S. and Chaikin, M., Some Aspects of Worsted-yarn Structure Part IV: The Application of Fourier Analysis to the Study of Single-fiber Configurations in a Series of Worsted Yarns, *J. Textile Inst.*, 1974, **65**, p. 537–551.
14. Morton, W.E., The arrangement of fibers in single yarns, *Textile Res. J.*, 1956, **26**, p. 325–331.
15. Morton, W.E. and Yen, K.C., The arrangement of fibers in fibro yarns, *J. Textile Inst.*, 1952, **43**, T60–T66.
16. Riding, G., Filament Migration in Single Yarns, *J. Textile Inst.*, 1964, **55**, T9–T17.
17. Evans, M., Hastings, N. and Peacock, B., *Statistical Distributions*, 3rd Edition, John Wiley & Sons, Inc., New York, 2000.
18. Schutz, R.A., Kueny, M., LeChatelier, J. and Hunzinger, S., New Type of Twist Determination for Open-end and Ring-spun Yarns, *Melliand Textilberichte International*, 1976, **57**, No. 6, 438–441.
19. Peirce, F.T., Theorems on the Strength of Long and Composite Specimens, *J. Textile Inst.* 1926, T335–368.
20. Backer, S., The Mechanics of Bent Yarns, *Textile Research Journal*., 1952, **22**, 668–681.
21. Brorens, P.H., Lappage, J., Bedford. J., Ranford, S.L., Studies on the Abrasion Resistance of Weaving Yarns, *J. Textile Inst.* 1990, **81**, (2) p. 126–134.
22. Choi, K.F., Wong, Y.W., Luo, Z.X. and Lam, Y.L., Measurement of Lateral Yarn Density Distribution Using Computer Tomography Principle, p. 57 *Proceedings of the 6th Asian Textile Conference Abstract Book*, paper file name: 58.pdf, Proceedings CDROM, Sept. 2001.
23. Choi, K.F. and Kim, K.L., Fiber Segment Length Distribution on Yarn Surface in Relation to Yarn Abrasion Resistance, *Textile Research Journal*, **74**, No. 7, p. 603–606.

12
Fabrics

Y. LI[1] AND X-Q. DAI[1,2]
[1]The Hong Kong Polytechnic University, China
[2]Soochow University, China

12.1 Characteristics and classification of fabrics

12.1.1 Woven fabric

According to the weave structure, woven fabrics are classified into *basic weave* fabrics, consisting of plain-woven fabric, twill fabric, and satin fabric; and *complex weave* fabrics, including leno fabric, crepe woven fabric, dobby fabric, Jacquard fabric and other fabrics of complicated structures.

The three basic weave fabrics are the most commonly used for garment materials. As shown in Fig. 12.1, in the plain weave, each warp yarn interlaces with each weft yarn to form the maximum number of interlacings; in twill weave, warp and weft yarns float over two or more yarns from the opposite direction in a progression of two to the right or left; and in satin weave, warp or weft yarns float over four or more yarns from the opposite direction in a progression of two to the right or left. Leno fabric is mesh-like, and its warp yarns have been made to cross one another between weft yarns during weaving. Dobby fabrics are fabrics with small woven-in geometric patterns. Jacquard fabrics are fabrics with intricate, detailed woven-in motifs.

12.1.2 Knitted fabric

In weft knits, the yarn forming the fabric traverses the fabric crosswise. There are four fundamental stitches forming the diversity of weft knits: knit stitch, purl stitch, float stitch and tuck stitch. The three basic *single weft knits* are jersey, rib and purl, which are composed of all knit stitches or of knit and purl stitch. These fabrics differ in appearance as well as mechanical performance due to their varying stitch structures. The incorporation of tuck and float stitches in the basic structure further introduces a variation of appearances and alters elongation and dimensions. The two *double knits* are rib and interlock, which are rib structures having alternating knit and purl stitches.

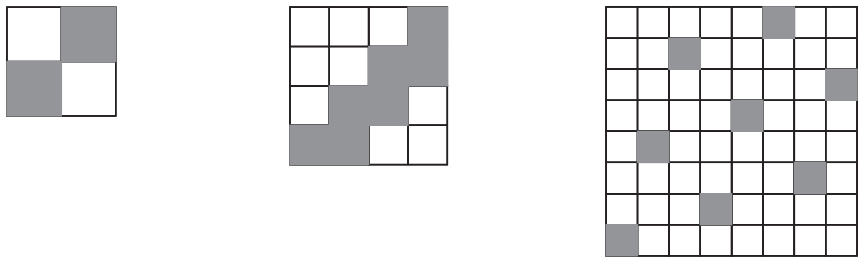

(a) Plain (b) Twill (c) Satin

12.1 Basic weaves.

In warp knits, the yarn forming the fabric traverses the fabric lengthwise. There are three major types of warp knits: tricot, Raschel, and nets and laces. *Tricot*, composed of all knit stitches, represents the commodity warp-knit product. Tricot fabrics vary in the number of sets of yarns in their structure: one-, two-, three- and four-bar. The greatest quantity of tricot produced is two-bar, which is used extensively in a variety of end uses.

Raschel knits are composed of vertical columns of chain stitches and an in-laid yarn that traverses the fabric horizontally between chain stitches. The three main types of Raschel fabrics are those with the basic structure, fall-plate Raschels, and pile Raschels. Both net and lace are open fabrics. Net is an open-mesh fabric in which a firm structure is ensured by some form of twist, interlocking, or knitting of the yarn. Lace is a fine openwork fabric with a ground of mesh or net on which patterns may be worked at the same time as the ground is formed or applied later, and which is made of yarn.

12.1.3 Functional fabrics

There are many kinds of functional requirements for fabrics, varying according to different garment end uses, such as easy care, softness of touch, quick drying, UV-protection, anti-bacteria, long durability, and so on. In regard to the mechanical performance of garments, fabric stretch and recovery are most important. In stretch fabric, a certain percentage of elastic fibers are usually incorporated.

12.2 Fabric construction measurement

Fabric length: The US standard ASTM D3773-90 and ISO 3933 describes the standard test methods for fabric length testing.

Fabric width: The width of a fabric depends on the loom on which the fabric is manufactured. Testing can follow the standard ASTM D3774 and ISO 3932.

Fabric thickness: This is one of the basic properties of a fabric, giving information on its warmth, heaviness, and stiffness in use. Since fabric is sensitive to the pressure used in thickness measurement, it is difficult to measure fabric thickness with satisfactory accuracy. Usually, a thickness gauge, micrometer, FAST-1[1] or KES-FB3[2] are used to obtain standard thickness or a thickness-pressure curve for a fabric. The standards ASTM D1777 and ISO 5084 describe several test methods for fabric thickness testing.

Fabric weight: The heavier a fabric, the more load that is placed on the human body wearing it. Weight can be conveyed as very light (<1 ounce per yard^2), light (2–3 ounces per yard^2), medium (5–7 ounces per yard^2), heavy (>7 ounces per yard^2), or very heavy. Fabric weight is usually measured by using a chemical balance. ASTM D3776, ISO 3801 and ISO 7211-6 describe several standard test methods for fabric weight.

Fabric weave: ISO 7211-1 describes the analysis method for fabric weave diagrams.

Fabric count: This is an important determinant of the quality of fabric and affects various mechanical properties. Generally, the higher the fabric count, the better the technological quality of the fabric. Fabric can also be roughly classified into: tightly woven, closely woven, and loosely woven. ASTM D3775-98 and ISO 7211-2 describe standard methods for determining fabric count.

Fabric crimp: This usually refers to yarn crimp in the fabric. It provides technological data for weaving design and for computation of yarn usage. ASTM D3883-99 and ISO 7211-3 describe the methods for determining yarn crimp in woven fabrics.

Yarn count and yarn twist: To analyze the construction of a fabric, the count and twist of yarn removed from fabric needs to be determined. ASTM D1059-97 and ISO 7211-5 are for testing the count of yarn removed from fabric, and the ASTM D1423-99 and ISO 7211-4 are for testing the twist of the yarn.

12.3 Basic mechanical properties and their measurement

12.3.1 Basic mechanical properties of fabric

In normal garment wear, cloth deformation is a mixture of tension, bending shearing and twisting. Therefore, besides the geometry and biomechanical properties of the human body, garment aesthetic appearance and mechanical comfort depends on these basic mechanical properties. Actually, fabric mechanical-comfort performance has been evaluated by consumers and textile producers subjectively by means of the hand of the fabric. And, fabric handle is used to describe the assessed results. However, fabric objective measurement (FOM) has been widely researched during the past several decades with the aim of specifying and controlling the quality, tailorability, and ultimate performance of apparel fabric. Many test methods, instruments and pieces of apparatus have been developed to measure parameters associated with fabric handle. Most of these parameters point to the basic mechanical properties of the fabric.

Tensile: Fabric tensile properties can be investigated on universal tensile testers. The most commonly used instrument for tensile test is the Instron tensile machine. A fabric specimen is often extended at a suitable rate of extension to its breaking point, and the load–extension curve is produced. There are two major ways to carry out the tensile test – strip test (BS 6176) and grab test (ASTM D1682), as illustrated in Fig. 12.2. Warp-wise and weft-wise specimens are prepared, then the tensile properties in these two principle directions can be investigated.

Figure 12.3 shows the load–elongation curves of two fabrics tested along the warp and weft directions on an Instron tensile machine. From these curves, the Young's modulus (that is the initial slope of the curve), break

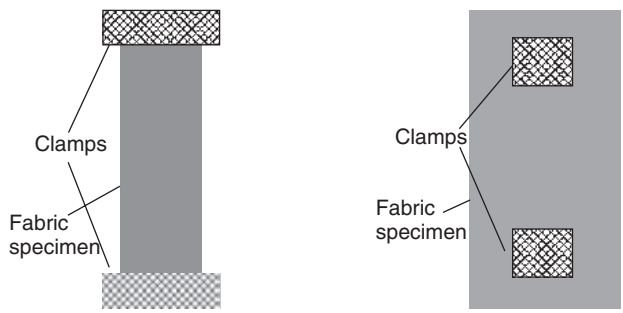

12.2 Instron tensile test.

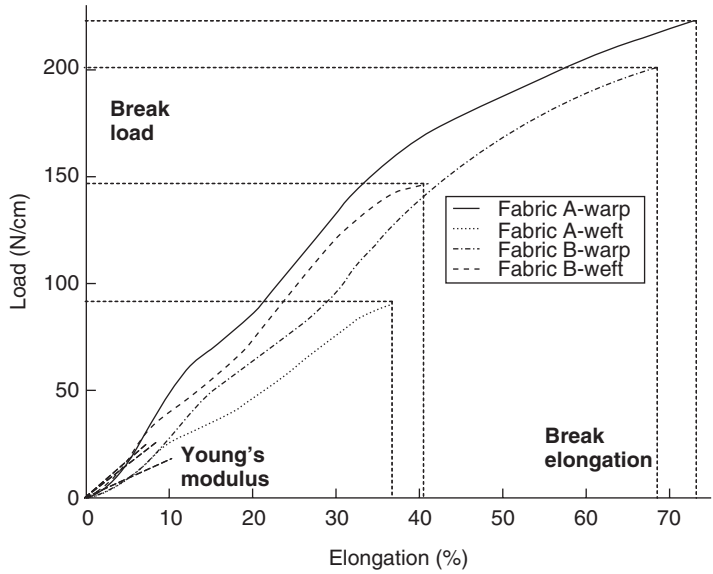

12.3 Instron load–elongation curves.

elongation and break load are often taken as parameters to describe the tensile properties of the fabrics tested. When extending a fabric specimen in one direction, it will contract in the other direction. The ratio of the contraction to the elongation is the Poisson ratio (σ). This can also be obtained by the biaxial tensile test.

Shear: It is the shear property that enables fabrics to undergo more complex deformations than two-dimensional bending and so conform to the contours of the body in garment end use. There are two major approaches to measure the shear property. One was proposed by Morner and Eeg-Olofsson,[3] the other one was developed by Behre.[4] Both of the two pieces of apparatus were attached to the Instron tester. Based on these two methods, many further investigations and improvements have been made.[5–8]

The resistance to shearing, R, is the same in the two methods:[6]

$$R = F - W\tan\theta = F - L\sin\theta.$$

Both of the two approaches produce records on a graph of the angular deformation and the resistance to deformation, and provide a complete hysteresis curve for the shear resistance of the fabric tested. Figure 12.4 shows a typical shear stress–strain curve. Cusick[5] took a number of parameters quantifying shear behavior from the curve: (i) the initial shear modulus, given by the slope of the curve at the origin O; (ii) the shear

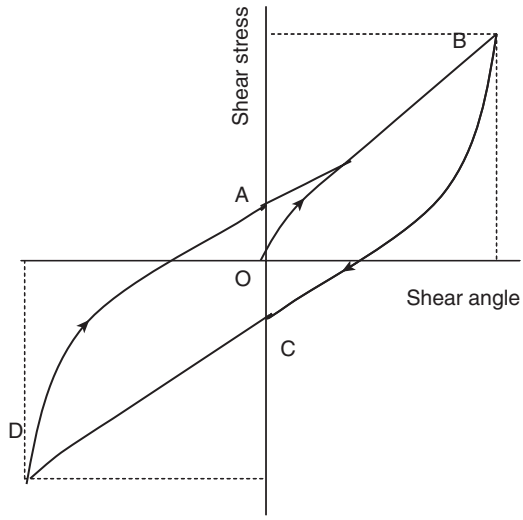

12.4 Typical shear curve.

modulus at zero shear angle, given by the slope at points A and B; (iii) the hysteresis at zero shear angle, given by the length of AC; and (iv) the buckling shear and the buckling angle at B and D, respectively.

Besides these items of apparatus/instruments designed specially for shear property investigations, there is also another approach to measure shear by using tensile testers directly. Killy has derived a formula that gives the Young's modulus (E_θ) for a fabric in the bias directions that are at an angle θ to the warp direction:[9]

$$1/E_\theta = (1/E_1)\cos^4\theta + (1/G - 2\sigma_1/E_1)\cos^2\theta\sin^2\theta + (1/E_2)\sin^2\theta\,.$$

Here, E_1 and E_2 are the Young's moduli of the warp and weft directions respectively, σ_1 denotes the Poisson ratio of the warp direction, and G is the shear modulus. If tensile tests are carried out on specimens of the warp, the weft, and the bias direction at an angle of 45° to the warp respectively, then the shear modulus G can be calculated by the above equation.

Bending: Since fabric stiffness has a dominant effect on aesthetic appearance in garment end use, there have been many methods developed to measure it. Peirce first proposed the Cantilever test.[10,11] In that test, a horizontal strip of fabric, one inch wide, is clamped at one end and the rest of the strip is allowed to hang under its own weight. The angle between the horizontal and the chord from the edge of the platform to the tip of the fabric is measured. He defined two quantities calculated from the angle θ:

(i) the bending length $c = l \cdot f(\theta)$, where l = length of fabric overhanging the platform(m), and $f(\theta) = \left(\frac{\cos 0.5\theta}{8 \tan \theta}\right)^{1/3}$;

(ii) the flexural rigidity $F = wc^3$ (Nm), where w = weight (g/m^2).

The higher the bending length, the stiffer the fabric. The Shirley stiffness tester measures the bending length of fabric in another way. A narrow horizontal strip (25 mm × 200 mm) of fabric is allowed to bend to a fixed angle under its own weight. The length of the fabric required to bend to this angle is taken as the bending length.

Peirce also proposed a hanging loop method for fabrics that are too limp to give a satisfactory result by the cantilever method.[10] A one-inch-wide strip of fabric of length L has its two ends clamped together to form loops of different shapes: ring, pear and heart. Figure 12.5 shows a heart loop. The undistorted length of the loop that is under no gravitational or other force, l_0, from the grip to the lowest point, has been calculated by Peirce. The actual length (l) of the loop under the force of gravity is measured. Then, the bending length is calculated as follows for each loop shape:

Ring loop: $l_0 = 0.3183L$, $\theta = 157°$ d/l_0, $c = L0.133f_2(\theta)$;

Pear loop: $l_0 = 0.4243L$, $\theta = 504.5°$ d/l_0, $c = L0.133f_2(\theta)/\cos 0.87\theta$;

Heart loop: $l_0 = 0.1337L$, $\theta = 32.85°$ d/l_0, $c = l_0 f_2(\theta)$.

Here, $d = l - l_0$, and $f_2(\theta) = (\cos\theta/\tan\theta)^{1/3}$. The flexural rigidity is calculated from the bending length in the same way as the cantilever test.

The stiffness of a fabric in bending is very dependent on its thickness, T; the thicker the fabric, the stiffer it is if all other factors are the same. The bending modulus, B (N/m^2), can then be calculated from the flexural rigidity by the following formula:

$$B = 12F/T^3.$$

ASTM D1388 and BS 3356 describe the details of fabric stiffness tests.

To investigate fabric stiffness, Owens *et al.* developed the Shirley cyclic bending tester.[12–15] A bending-hysteresis curve can be obtained from this.

Twist: Since fabric twist always occurs accompanied by bending, it is difficult to measure the pure twist of fabric. Shanahan *et al.* have pointed out that a pure bending along a bias direction is a combination of twist and bending in the warp and weft directions.[16] A formula was derived to calculate the flexural rigidity in the bias direction at an angle θ to the warp:[18]

$$F_\theta = F_1 \cos^4\theta + (4\tau + 2\upsilon_2 F_1)\cos^2\theta \sin^2\theta + F_2 \sin^4\theta$$

where, F_1 and F_2 denote the flexural rigidities in the warp and weft direction, υ_2 is analogous to Poisson's ratio, and τ is the twist rigidity. Then, instead of

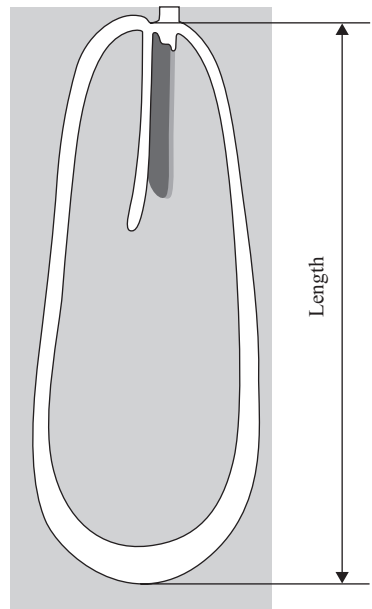

12.5 Heart loop.

measuring twist rigidity directly, it can be obtained by testing the bending of a fabric specimen in a bias direction. With F_1, F_2 and F_θ known, the twist rigidity can be obtained.

Compression: The Schiefer compressometer and universal testers with compression cells can be used to obtain the thickness–pressure curve. ASTM D 6571 discloses a method to measure the compression resistance and recovery properties of any type of high-loft, non-woven fabric using a simple and economically applied static weight loading technique.

Table 12.1 provides a summary of the basic mechanical property tests.

Table 12.1 Summary of basic mechanical property tests

Property	Instruments/methods	Parameter description	Units	References
Tensile	Universal/tensile testers(Instron, Hounsfield, etc.)	Load-elongation curve, Extensibility, Initial Young's modulus, Recovery, Hysteresis	– % N/m width % N/m width	[10]
Shearing	Universal/tensile testers(bias extension) Morner and Eeg-Olofsson's method, Behre's method	Load-extension curve in bias direction, Shear-force/shear-angle curve, Shear modulus, Shear hysteresis	– – N/m*degree N/m	[3–5, 19]
Bending	Cantilever, Hanging loop, Shirley stiffness tester, Shirley cyclic bending tester	Bending length, Felxural rigidity, Bending modulus, Bending hysteresis curve	mm Nm N/m^2	[10, 11, 13–15, 17, 20, 21]
Compression	Universal testers(compression cells), Schiefer compressometer	Thickness-pressure curve, Compressibility, Compressional resilience and hysteresis	– %	[10] [23]

12.3.2 Surface properties

As described in Chapter 9, the basic mechanical properties have an influence on a garment's aesthetic appearance as well as contact comfort through pressure. Besides them, the surface properties (usually roughness and friction) of cloth influence not only the contact state, but also the touch sense of humans. A number of roughness testers have been used for measuring the surface roughness of sheet materials.[13]

There are several approaches for fabric friction measurement. One approach is to carry out friction tests in tensile testers with special friction attachments. The principle of the test is illustrated in Fig. 12.6a, where a block of mass m is pulled over a horizontal flat rigid surface covered with the fabric being tested, and the line connected to the block is led around a frictionless pulley and connected to an appropriate load cell in a tensile tester. Then, the coefficient of friction, $\mu = F/mg$. The Instron machine is most popularly used.[13] An inclined plane method, illustrated in Fig. 12.6b, has also been used for fabric friction testing. Here, $\mu = \tan\theta$. The Shirley Fabric Friction Tester was developed for testing coated fabrics based on this principle.[18]

12.3.3 KES-F system

Kawabata and his co-workers developed the KES-F (Kawabata Evaluation Systems for Fabrics) with the aim of objectively measuring the appropriate fabric properties and then correlating these measurements with the subjective assessment of handle.[19] The system consists of four specialized instruments: (i) FB1 tensile and shearing; (ii) FB2 bending; (iii) FB3 compression; and (iv) FB4 surface friction and variation. The system investigates the responses of various mechanical behaviors under low-load. As is well known, fabric mechanical properties in the low-load region possess a pecu-

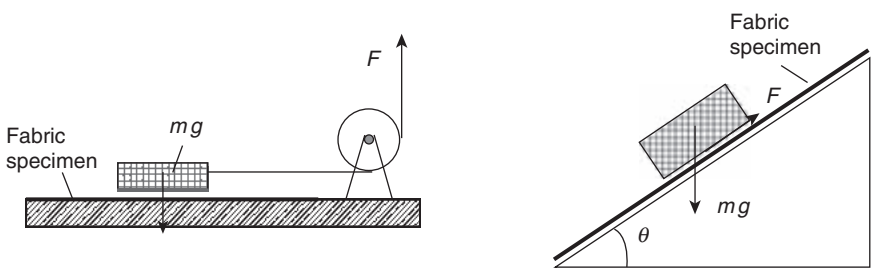

(a) Horizontal pull (b) Friction inclined plane

12.6 Friction test.

liar non-linearity. One example of the non-linearity is the hysteresis behavior in the load–deformation relation. These properties of cloth have significant influences on the aesthetic shape and wear comfort in garment end use. They must be measured exactly and expressed by parameters. Fabric specimens of 20 cm × 20 cm are used for all measurements except compression.

Tensile property

The tensile test is illustrated in Fig. 12.7a. Extension is applied along the 5 cm direction of the specimen up to 500 gf/cm. The transverse contraction is not limited, so the test is a type of biaxial extension. Figure 12.7b shows a typical load–extension hysteresis curve. From this curve, several parameters are derived:

Tensile energy, $WT = \int_0^{\varepsilon_m} F\mathrm{d}\varepsilon$ (gf×cm/cm^2);

Linearity of load–extension curve, $LT = WT/WOT$, where $WOT = F_m \cdot \varepsilon_m/2$;

Tensile resilience, $RT = (WT'/WT) \times 100$, (%), where $WT' = \int_0^{\varepsilon_m} F'\mathrm{d}\varepsilon$;

Extensibility, EM, the strain (ε_m) at 500 gf/cm.

Shearing property

The shear test is carried out using the same tester as the tensile test (KES-FB1). It is illustrated in Fig. 12.8a; a rate of shear strain of 8.34×10^{-3}/sec is applied to the specimen under a constant extension load (10 gf/cm) up to a maximum shear angle of 8°. Figure 12.8b is the obtained shear-force/shear-angle hysteresis curve. From it, the following parameters are measured:

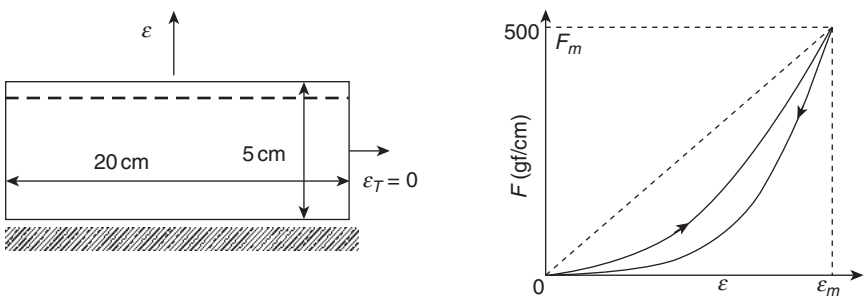

(a) Specimen extension (b) Load–elongation curve

12.7 KES tensile test.

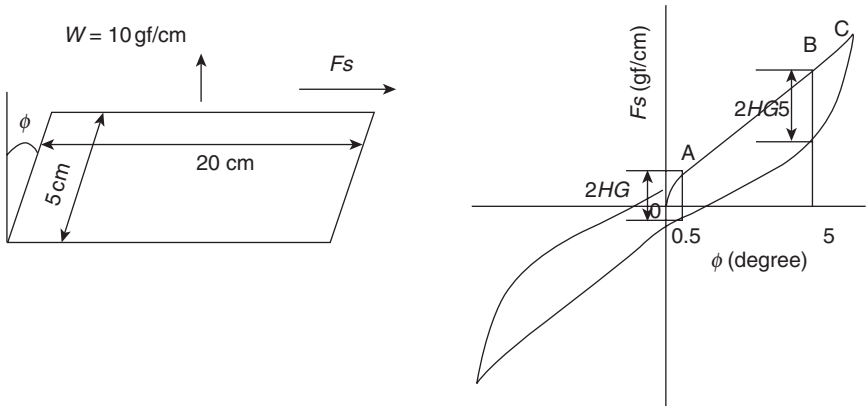

(a) Specimen shearing (b) KES shearing curve

12.8 KES shear test.

(i) G, shear rigidity, mean slope of the curve in the region $\phi = 0.5° \sim 5°$; (ii) $2HG$, hysteresis of shear force at shear angle of 0.5°; (iii) $2HG5$, hysteresis of shear force at shearing angle of 5°.

Bending

Figure 12.9 shows the KES-FB2 bending tester. In the KES bending test, a specimen is bent between the curvatures –2.5 and 2.5 cm^{-1}, as illustrated in Fig. 12.10a. Figure 12.10b is a bending curve, from which two parameters are measured: B, bending rigidity, the mean slope of the curve in the region $K = 0.5 \sim 1.5\,cm^{-1}$; and $2HB$, hysteresis of bending moment, measured at $K = 0.5\,cm^{-1}$.

Compression

Figure 12.11 shows the KES compression tester FB3. The specimen used for the compression test is 2.5 cm × 2.0 cm and the effective pressure region is a circular area of 2 cm^2. The specimen is compressed in the direction of its thickness to a maximum pressure of 50 gf/cm^2, as illustrated in Fig. 12.12a. The shape of the obtained pressure–thickness curve (Fig. 12.12b) is similar to that of the load–extension curve, and the parameters are also defined the same way as those for the tensile property: LC, linearity of compression curve; WC, compression energy; and RC, compression resilience. The fabric thickness at 50 Pa pressure, T_0 and that at 200 Pa pressure T_m can also be obtained from the thickness–pressure curve. The compression tester can also be used for fabric thickness measurement.

12.9 KES-FB2 bending tester.

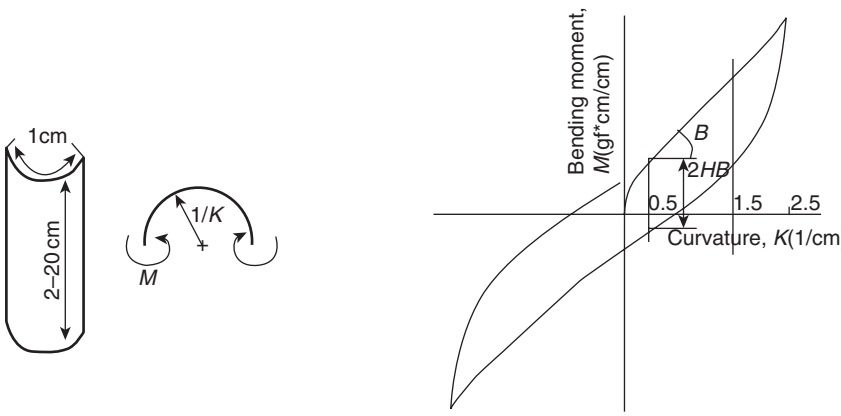

(a) Specimen bending (b) KES bending curve

12.10 KES bending test.

Surface properties

Figure 12.13 is the KES-FB4 tester for evaluating surface properties. Surface roughness is measured by pulling across the surface a steel wire of 0.5 mm diameter that is bent into a U shape, as illustrated in Fig. 12.14a. Figure

12.11 KES-FB3 tester.

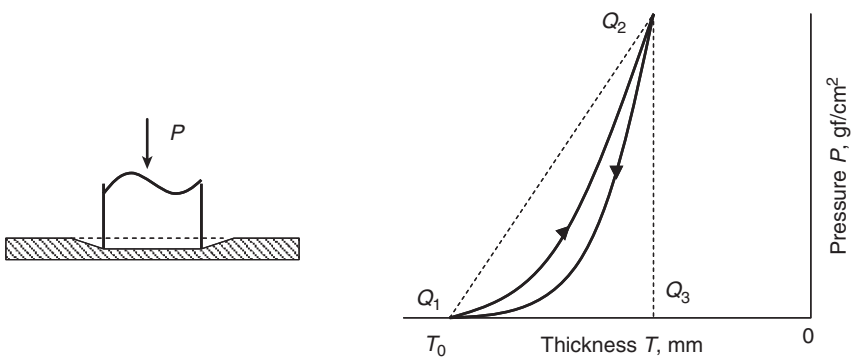

(a) Compression deformation (b) KES compression curve

12.12 Compression test.

12.14b shows a plot of the height variation along the distance. The mean deviation of surface contour, *SMD* is calculated from the plot, *SMD* = hatched area/*X*.

Surface friction is measured in a similar way by using a contactor consisting of 10 pieces of the same wire used in the roughness test, as shown in

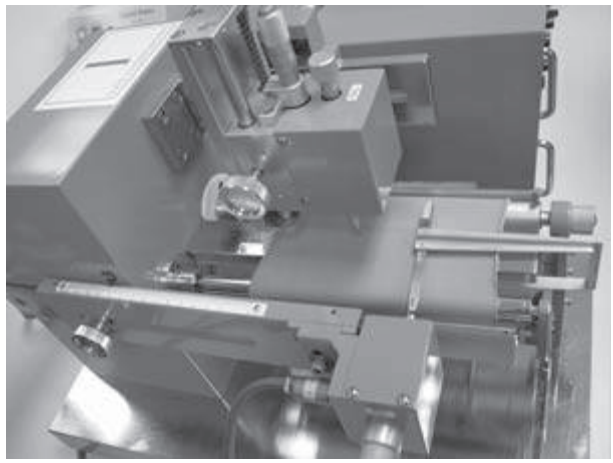

12.13 KES-FB4 tester.

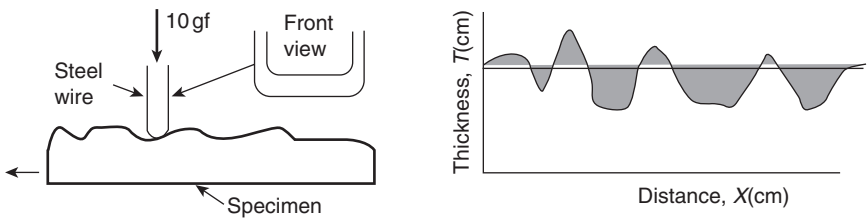

(a) Roughness measurement (b) Surface thickness variation

12.14 KES surface roughness test.

Fig. 12.15a. The force required to pull the fabric passing the contactor is measured. Figure 12.15b shows the obtained plot of friction versus distance travelled, from which two parameters are calculated: the coefficient of friction, *MIU*, the mean value of the curve; and the mean deviation of the coefficient of friction, *MMD*.

12.3.4 The FAST system

Fabric Assurance by Simple Testing (FAST) is a system specifically designed by CSIRO in Australia for use by tailors and worsted finishers to highlight problems that may be encountered in making fabrics, mainly wool and wool-blend, into garments.[1] It is claimed to be much simpler and more robust than the KES-F system, so it can be used as an alternative in many applications. This system comprises three purpose-designed instruments: FAST 1, compression meter, FAST 2, bending meter, and FAST 3, extension

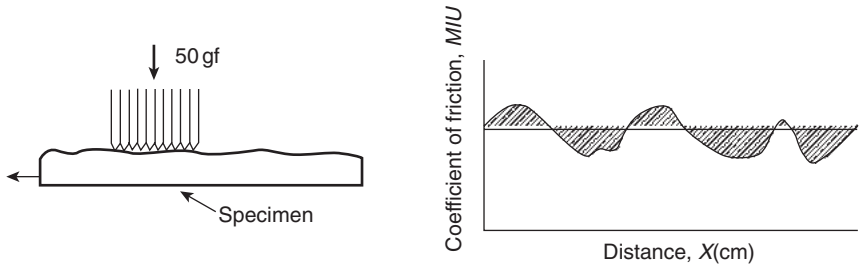

(a) Friction measurement (b) Surface friction variation

12.15 KES surface friction test.

meter; and a test method, FAST 4, dimensional stability test, which requires no specialized equipment.

In the compression test, the thickness of a fabric specimen is measured on a 10 cm^2 area at two different pressures, firstly at 2 gf/cm^2 (0.196 kPa) and then at 100 gf/cm^2 (9.81 kPa). The difference between these two thickness values is regarded as the fabric surface thickness. This is based on the consideration that a fabric consists of an incompressible core and a compressible surface.

The FAST bending meter measures the bending length of a fabric specimen automatically. The flexural rigidity is then calculated from the bending length and the fabric weight as mentioned before.

Using the FAST extension meter, the extension of the fabric is measured in the warp and weft directions at three fixed forces – 5, 20, 100 gf/cm (4.9, 19.6, and 98.1 N/m). The extension at 98.1 N/m is defined as the extensibility. And the extension values at 4.9 and 19.6 N/m are measured for the calculation of the formability, together with the respective bending rigidity. The extension is also measured on the bias in both directions, only at a force of 5 gf/cm (4.9 N/m), to enable the calculation of the shear rigidity.

12.4 Mechanical properties in complex deformation

12.4.1 Bi-extension

In normal garment wear, especially with tight-fit garments, the fabric is often stretched in both the two principal directions. How the fabric responds to such deformation has an important influence on the appearance and comfort of the garments. Kawabata *et al.* developed an instrument to investigate the fabric properties in biaxial extension. Figure 12.16 shows the KES-G2 tester. The test is illustrated in Fig. 12.17a, where two forces are applied continuously to the two axes of the fabric specimen,

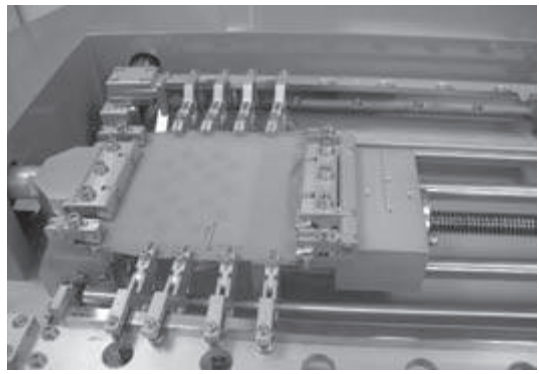

12.16 KES-G2 tester.

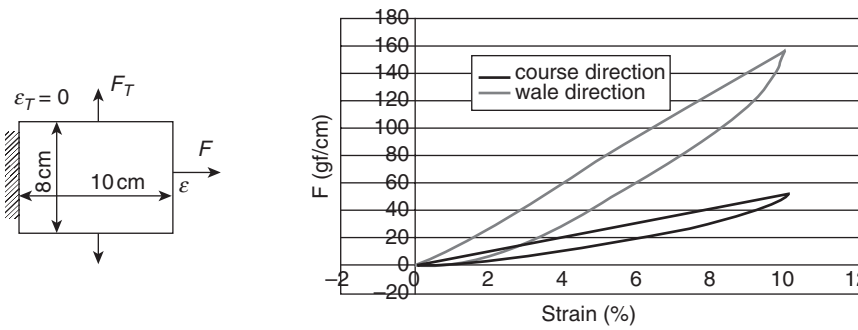

(a) Specimen biaxial extension (b) Load–extension curve

12.17 KES biaxial tension test.

respectively, to keep it constrained on one axis and elongated on the other axis. Figure 12.17b shows the obtained curve of the two forces versus the elongation.

12.4.2 Buckling and formability

Eeg-Olofsson developed a method to measure fabric plate buckling using an Instron tensile testing machine.[21] The test specimen was inserted between two clamps. The lower clamp was rigidly fixed to the movable Instron beam. The upper clamp was guided by means of two rods mounted in bearings on the frame of the Instron machine and suspended by a wire from the strain-gauge. An extra load was hung on the left-hand of the rods in order to maintain tension in the suspension wire throughout the test.

Dahlberg also developed an apparatus as an attachment to the Instron tensile tester for measuring plate buckling and shell buckling of fabric.[22] Both of the tests produced load–deformation curves.

Formability is a measure of the degree of compression in the fabric plane sustainable by it before buckling occurs. Lindberg *et al.* pointed out that it is an important property required in garment construction.[23] Low values of formability indicate that a fabric becomes easily puckered when made into a collar or cuff. The compression force required to buckle a sample of fabric of length l is given by $P = kB/l^2$, where B is the bending rigidity, and k is a constant. Under this compression force, the amount of the fabric compression before it buckles is then given by $CP = kCB/l^2$, where C denotes the longitudinal compressibility (that is often assumed to be equal to the extensibility). Here, CB is a specific property of the fabric determining how much compression it can undergo before buckling. It is defined as the compression formability, F_c.[23] There is no particular instrument for the formability test. It is usually a by-product of the measurements of tensile modulus and bending rigidity.

12.4.3 Drape

The British standard for the assessment of drape of fabrics (BS 5058) describes a method using the 'Drapemeter'. A circular specimen, about 0.3 m in diameter, is supported on a circular disk of 0.18 m diameter. The unsupported area may drape to form some folds. The number of the folds (nodes) is used to describe the drapability directly. The more the nodes, the softer is the fabric. The drape coefficient is the ratio of the projected area of the fabric sample to its undraped area, in which the area of the supporting disk is deduced.

> Drape coefficient = (the area of the shadow – the area of the supporting disk)/(the area of the circular specimen – the area of the supporting disk)

The higher the drape coefficient, the stiffer the fabric.

According to BS 5058, there are three diameters of specimen that can be used:

(i) 30 cm for medium fabrics;
(ii) 24 cm limp fabrics, whose drape coefficients are below 30% with the 30 cm sample;
(iii) 36 cm for stiff fabrics, whose drape coefficients are above 85% with the 30 cm sample.

12.4.4 Stretch and recovery properties

Certain types of garments, particularly sportswear, dancewear, and foundation underwear, are made to be close-fitting or tight-fitting to the body. The fabric for such garments should be able to stretch to accommodate firstly the donning and removal of the garment and secondly any activity that is undertaken while wearing it. To avoid bagging and to remain close fitting, the stretch has to be followed by complete recovery of the original dimensions. For this purpose, usually a small percentage of elastic fibers are incorporated into the fabric structure. There are a large number of methods developed for stretch fabric measurement. Generally, two quantities are measured: one is the extension at a given load, sometimes known as the modulus, which is a measure of how easily the fabric stretches; the other is how well the fabric recovers from stretching to this load, usually measured as growth or residual extension.[24]

The British standard for elastic fabrics (BS 4952) describes a number of test methods using either line contact jaws or looped specimens. The standard covers both woven and knitted fabrics. The measured quantities include: extension at a specified force, modulus, residual extension and tension decay. In the extension test, the sample is cycled twice between zero extension and a specified force. The elongation at the specified force is measured for the extension, and the modulus is obtained by recording the force at specified values of elongation. In the residual extension test, the sample of gauge length L_1 is given a preliminary stretch cycle then extended by a specified force that is held for 10 s. The force is then removed and the sample is allowed to relax on a flat and smooth surface. The length of the sample clamped between the jaws is measured after 1 min (L_2) and after 30 min (L_3) respectively. The following quantities are calculated:

$$\text{Mean residual extension after 1 min} = \frac{L_2 - L_1}{L_1} \times 100\%,$$

$$\text{Mean residual extension after 30 min} = \frac{L_3 - L_1}{L_1} \times 100\%.$$

The tension decay is tested by holding the sample at a specified elongation for 5 min and measuring the decay in force over this period: Tension decay = $\frac{F_1 - F_2}{F_1} \times 100\%$, where F_1 is the maximum force at the specific elongation, and F_2 is the force after 5 min.

The US standard for the stretch properties of woven stretch fabric (ASTM D3107) measures two quantities: percentage stretch, elongation at a fixed

load; and fabric growth, which is the same as residual extension. The US standard for knitted fabric having lower power (ASTM D2594) measures the stretch and the growth after a much longer period.

12.4.5 Strength

Bursting strength

Tensile strength tests are generally used for woven fabrics where there are definite warp and weft directions. However, some other fabrics, such as knitted fabrics, lace or non-woven fabrics do not have such principle directions where the strength reaches a maximum. Bursting strength, in which the material is stressed in all directions at the same time, is an alternative method of measuring strength for such materials. Actually, in many garments, especially at some particular position, such as elbows and knees, the fabric is stressed in all directions during wearing, so it is important to carry out a strength test in a realistic manner.

The BS 4768 describes a diaphragm bursting strength test method, as illustrated in Fig. 12.18a. The fabric specimen is clamped over a rubber diaphragm by means of an annular clamping ring and an increasing fluid pressure is applied to the underside of the diaphragm until the specimen bursts. The operating fluid can be a liquid or a gas. Two quantities are reported: mean bursting strength (kN/m^2) and mean bursting distension (mm). ASTM D3786 describes a similar method. ASTM D3787 describes a ball bursting strength method as illustrated in Fig. 12.18b. The test can be carried out using an attachment on a standard tensile testing machine. In

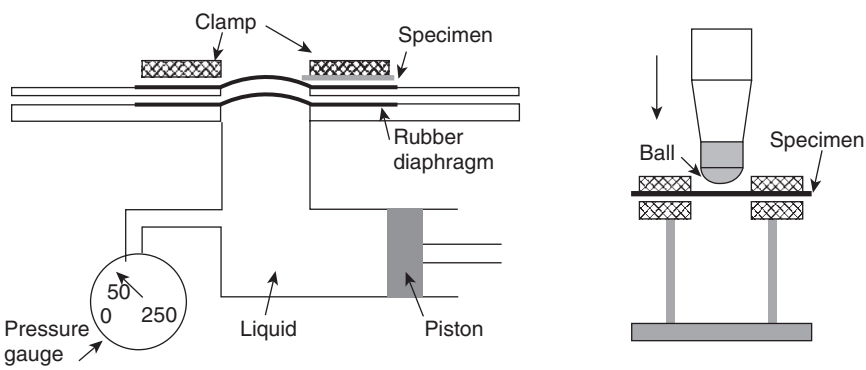

(a) Diaphragm bursting strength (b) Ball bursting strength

12.18 Bursting test.

the test, a steel ball is pushed through the stretched fabric specimen and the force required is recorded. ISO 13938 also describes a hydraulic method and a pneumatic method for determination of bursting strength and a bursting distension.

Tearing strength

A fabric tears when it is snagged by a sharp object and the immediate small puncture is converted into a long rip by what may be a very small extra effort. It is the most common type of strength failure of fabrics in end use. For garment items, such as outdoor clothing, overalls and uniforms, the tearing strength is a very important quantity. The fabric tear property measured is the force required to propagate an existing tear and not the force required to initiate a tear, as this usually requires cutting of threads. In the test, the specimen is cut first and the force required to extend the cut is measured. This is conveniently carried out by gripping the two halves of the cut in a standard tensile tester, and obtaining a tear test force extension curve. The various tear tests carried out in this manner, which are called tongue tear tests, differ mainly in the geometry of the specimen. ASTM D2261 describes a single rip tear test method, and BS 4303 also describes a wing rip tear test method. The results can be expressed as the maximum, the median, or the average tearing resistance.

Another approach to measure tear strength is the ballistic tear test, which measures energy loss (work done) during tearing. ASTM 1424 describes a tear strength test using the Elmendorf tear tester. There is the following equation for the relationship between the tearing force and the energy loss:

$$\text{Energy loss} = \text{tearing force} * \text{distance}.$$

Seam strength

Seam strength is the resistance to yarn slippage in a fabric seam. There are three different types of seam slippage test:

(i) To measure the maximum force to seam rupture.
(ii) To plot a load–extension curve with and without a standard seam and take the difference between the two curves as the slippage.
(iii) To put a standard seam under a fixed load and measure the seam gape.

ISO 13935 describes two methods of the first type. BS 3320 describes a standard test of the second type.

12.4.6 Bagging

There are a few methods developed for evaluation of woven and knitted fabrics' bagging behavior. The Celanese bagging test uses the principle of tensile stretch and recovery and is adaptable to the Instron tensile machine.[25] A 10-inch-diameter specimen is subjected to repeated loads of between 0.5 and 15 pounds. The immediate growth and immediate distortion are recorded, and from them a measure of immediate recovery is obtained. Based on a comparison with wear trials, fabrics with an immediate recovery value greater than 59% are considered to be satisfactory, 53–59% to be on the borderline and less than 53% to be unsatisfactory.

The Zweigle type bagging tester uses the Gronewald and Zoll principle, and enables measurement of bagging tendency under reasonably realistic conditions.[26] The testing apparatus is an artificial arm with an elbow joint. The test fabric, suitably made into tubular form, is drawn onto the tester. With the testing arm bent, the sample is subjected to five hours of static strain. The testing arm is then brought to the straight position and the specimen is allowed to recover. After a 10-minute recovery, the specimen is withdrawn from the arm and the bagging height at the elbow region is measured. For all the fabrics tested, when the bagging height measured in the laboratory was below 5 mm, a fabric was judged to be wearable under practical conditions.

Yokura *et al.*[27] developed an apparatus for the measurement of fabric bagging behavior in terms of increased volume. In the test, a fabric sample is placed on a hemisphere of 14 cm diameter, clamped by chucks and then loaded using a square frame for five hours. The shape of the distorted specimen is measured using the Moiré topographic technique. The volume formed by the bagged fabric is used to evaluate its bagging propensity.

Zhang[28] and Zhang *et al.*[29,30] developed an apparatus that is attached to an Instron tensile machine to investigate the dynamic bagging property of a fabric. A specimen, under a pre-tension force, is stretched to a predetermined height and returned to its original position. This process is repeated continuously many times, followed by a specified recovery time under zero loading. After recovery, the specimen is subjected again to the same pre-tension force and then the non-recovered bagging height is measured. The relative residual bagging height is then the ratio of the non-recovered bagging height to the predetermined bagging height in percentage terms.

12.5 Conclusion

The structural features, classification of woven and knitted fabrics, and the fabric construction measurements have been briefly reviewed. Descriptions of the mechanical properties of fabrics in simple and complex deformations,

which determine the biomechanical performance of clothing, were introduced. The commonly used parameters were derived from these descriptions. To obtain these parameters for biomechanical engineering design, various testing methods and apparatus including the KES and FAST systems were summarized.

12.6 Acknowledgement

We would like to thank Hong Kong Polytechnic University for funding this research through Projects A188 and G-YD31.

12.7 References

1. De Boos, A.G. and Tester, D.H., The FAST Approach to Improved Fabric Performance, in *First International Clothing Conference*. 1990. Braford.
2. Kawabata, S., The Development of the Objective Measurement of Fabric Handle, in *Second Australia–Japan Symposium on Objective Evaluation of Fabric Quality, Mechanical Properties, and Performance*. 1982. Kyoto: Textile Machinery Society of Japan.
3. Morner, B. and Eeg-Olofsson, T., Measurement of the Shearing Properties of Fabrics. *Textile Research Journal*, 1957. **27**(8): p. 611–615.
4. Behre, B., Mechanical Properties of Textile Fabrics, Part I: Shearing. *Textile Research Journal*, 1961. **31**(2): p. 87–93.
5. Cusick, G.E., The Resistance of Fabrics to Shearing Forces: A Study of the Experimental Method due to Morner and Eeg-Olofsson. *Journal of the Textile Institute*, 1961. **52**: p. T395–T406.
6. Treloar, L.R.G., The Effect of Test-Piece Dimensions on the Behaviour of Fabrics in Shear. *Journal of the Textile Institute*, 1965. **56**: p. T533.
7. Spivak, S.M., The Behavior of Fabrics in Shear, Part I: Instrument Method and the Effect of Test Conditions. *Textile Research Journal*, 1966. **36**: p. 1056–1063.
8. Koh, V.K., Shear Behavior of Woven Fabrics. *Textile Research Journal*, 1989. **59**: p. T142–T150.
9. Killy, W.F., Planar Stress–Strain Relationships in Woven Fabrics. *Journal of the Textile Institute*, 1963. **54**: p. T9–T27.
10. Peirce, F.T., The Handle of Cloth as a Measurable Quantity. *Journal of the Textile Institute*, 1930. **21**: p. T377.
11. Abbott, N.J., The Measurement of Stiffness in Textile Fabrics, Part II: A Study of the Peirce Cantilever Test for Stiffness of Textile Fabrics. *Textile Research Journal*, 1951. **21**(6): p. 441–444.
12. Livesey, R.G. and Owens, J.D., Cloth Stiffness and Hysteresis in Bending. *Journal of the Textile Institute*, 1964. **55**: p. T516.
13. Owens, J.D., An Automatic Cloth-bending-hysteresis Tester and Some of its Applications. *Journal of the Textile Institute*, 1966. **57**: p. T435–T438.
14. Owens, J.D., *Journal of the Textile Institute*, 1967. **58**: p. 589.
15. Owens, J.D., *Journal of the Textile Institute*, 1968. **59**: p. 313.

16. Shanahan, W.J., Lloyd, D.W. and Hearle, J.W.S., Characterizing the Elastic Behavior of Textile Fabrics in Complex Deformation. *Textile Research Journal*, 1978. **48**(4): p. 495–505.
17. Cooper, D.N.E., The Stiffness of Woven Textiles. *Journal of the Textile Institute*, 1960. **51**: p. T317–T335.
18. Shirley Institute, *Shirley Fabric Friction Tester(SDL 264), Instruction Manual* (Date unknown).
19. Kawabata, S., The Standardization and Analysis of Hand Evaluation, The Textile Machinery Society of Japan. 1980.
20. Kawabata, S. and Niwa, M., Objective measurement of fabric hand, in *Modern Textile Characterization Methods*, M. Raheel, Editor. 1996, Marcel Dekker, Inc.
21. Eeg-Olofsson, T., *Journal of the Textile Institute*, 1959. **50**: p. T112–T132.
22. Dahlberg, B., Mechanical Properties of Textile Fabrics, Part I: Buckling. *Textile Research Journal*, 1961. **31**(2): p. 94–99.
23. Linberg, J., Waesterberg, L. and Svenson, R., Wool Fabrics as Garment Construction Materials. *Journal of the Textile Institute*, 1960. **51**: p. T1475.
24. Slater, K., Chapter 5, Strength and Elongation Tests, in *Physical Testing and Quality Control*. The Textile Institute, Manchester, 1993.
25. Thomas, W., Celanese Bagging Test for Knit Fabrics. *J. Am. Assoc. Textile Chemists and Colorists* 1971. **3**: p. 231–233.
26. Gronewald, K.N. and Zoll, W., Practical Method for Determining the 'Bagging' Tendency in Textiles. *International Textile Bulletin, Weaving*, 1973. **3**: p. 273–275.
27. Yokura, H., Nagae, S. and Niwa, M., Prediction of Fabric Bagging from Mechanical Properties. *Textile Research Journal*, **105**: p. 748–754.
28. Zhang, X., Mechanism of Woven Fabric Bagging, in *Institute of Textiles and Clothing*. 1999, PhD Thesis, The Hong Kong Polytechnic University: Hong Kong.
29. Zhang, X. *et al.*, Fabric Bagging, Part I: Subjective Perception and Psychophysical Mechanism. *Textile Research Journal*, 1999. **69**(7): p. 511–518.
30. Zhang, X. *et al.*, Fabric Bagging, Part II: Objective Evaluation and Physical Mechanism. *Textile Research Journal*, 1999. **69**(8): p. 598–606.

13

Human skin and underlying soft tissues

M. ZHANG AND J.T. CHEUNG
The Hong Kong Polytechnic University, China

13.1 Introduction

In this chapter, common experimental techniques to quantify the tensile, compression, shear and frictional properties of the human skin and underlying tissues are reviewed. Selected material properties of the human skin tissues are highlighted.

13.2 Biomechanical testing of human skin

Many biomechanical approaches have been developed to test the human skin and underlying tissues. The aims are not only to understand the tissues distinct behaviors, but also to help in clinical diagnosis of skin diseases. Noninvasive measurements of skin mechanical properties provide a possibility for monitoring the temporal effects of disease, drugs, or cosmetics within and across subjects. Establishing objective and quantitative measurements of skin properties is one important aspect for clinical treatment and diagnosis.

Due to the structural variations, the mechanical properties of skin may vary with the subject, body site, direction, testing condition such as strain rate, and ambient conditions. An ideal test should be conducted *in vivo* with controlled specimen size and condition, such as multiaxial tests with uniform strain fields, so that the skin comprehensive properties can be readily associated with the results.[1] However, this can hardly be achieved because it is difficult to obtain a uniform strain field throughout the testing area and to control the loading boundaries in *in vivo* tests. There are difficulties in measuring the resting tension and deformation, the skin dimension and the boundary effects. These difficulties can be solved in an *in vitro* test but the effects of biological behaviors, such as blood pressure, lymphatic drainage, metabolism, and nervous and hormonal controls may be lost. Although *in vitro* testing based on standardized methods can give more repeatable results, *in vivo* skin properties are more relevant to clinical application and

in the fields of textiles and clothing. However, interpretation of *in vivo* tests is difficult because of the measurement constraints and indifferentiable response from boundary and underlying soft tissues.

13.2.1 *In vitro* tests of human skin

An *in vitro* test means that the skin specimen is tested away from the body. *In vitro* methods involve the removal of skin samples from the body and the usual procedure is to excise the skin and to pare off as much subcutaneous fat as possible. Therefore, the tissue cannot be further modulated in *in vivo* situations and thus a significant amount of series measurements of samples from different sites are required for adequate interpretation of results. *In vitro* uniaxial tests or strip biaxial tests are well suited for studies of the anisotropic behavior of the skin because of their better strain uniformity than *in vivo* tests.

The site and orientation of the tested specimen are very important, as anisotropic pre-existing or resting tension of skin exists as a result of structural strain, normal habitual body movements, and underlying joints or musculature. The sample is cut into a dumbbell shape, with the middle portion considered as the test site, and the larger ends are gripped on a tensile testing machine. In this arrangement, the specimen can be stretched under a uniform strain field throughout the skin thickness. It should be noticed that repeating the application of test stresses in both *in vitro* and *in vivo* tests is essential to allow a steady-state response to be achieved, leading to good reproducibility of results.

The ultimate strength and elastic parameters are commonly extracted from *in vitro* mechanical testing of skin. Edwards and Marks[2] summarized the results of selected *in vitro* tests of normal human skin samples of dimensions 4 mm × 2 mm × skin thickness of approximately 1–2 mm. The tensile strength of skin ranged from 5 to 30 N/mm^2, with a maximum mean value of about 21 N/mm^2 at 8 years, declining to about 17 N/mm^2 at 95 years. The ultimate modulus of elasticity ranged from about 15 to 150 N/mm^2. The mean showed a maximum value of about 70 N/mm^2 at age 11, with a decline to about 60 N/mm^2 at 95 years. The ultimate strain varied from about 35 to 115%. The mean value declined in a linear fashion from 75% at birth to 60% at 90 years.

13.2.2 *In vivo* tests of skin

An *in vivo* test means that the skin is tested on body. Though it is difficult to extract consistent mechanical parameters for inter and intra studies comparison, it can provide important information on functional skin mechanics. In fact, the *in vivo* tests have been widely used for the objective

assessment of severity and response to treatment in several diseases. In the following sections, the common measuring techniques and devices for *in vivo* testing of the human skin are discussed.

Tensile test (extensometer, twistometer, cutometer)

Extensometer: The simplest method for measuring the tensile properties of skin is the use of a linear uniaxial extensometer. Tabs are attached to the skin with either cyanoacrylate glue or double-sided adhesive tape and are driven apart to give a preset extension of typically 30%.[2] Strain gauges and a linear variable differential transformer sensor (LVDT) are attached to measure the forces applied to the pads and their displacements.[3] The force required to stretch the skin and maintain the new tab separation can be recorded. Alternatively, the separation of the tabs can be monitored with the application of a constant extension force. This cannot easily be achieved *in vivo*, but a good approximation can be obtained by using attachment tabs that are much wider than their initial separation distance. In this configuration, the skin is prevented from necking in the region of strain application and therefore experiences an effective stress in a direction orthogonal to the extension axis. Modulation of stratum corneum properties by as much as 30% from the effects of emollient applications and different tissue disorders can be evaluated.[2] This method can also be used to study changes due to aging, radiation therapy, steroid application and plastic surgery. Testing of skin properties using the extensometer is practically convenient; however, a pure uniaxial tensile test cannot be achieved as the specimen boundary conditions are not well defined.

Table 13.1 highlights some of the measured material parameters of skin using uniaxial extensometers, in the literature. The uniaxial extensometer has been employed to help evaluate the treatment of postburn hypertrophic skin[4] and the effects of aging and photodamage under sun exposure.[5]

Twistometer: The in-plane response of skin to a torsional stimulus can be measured by a twistometer, which has a central disk within a thin annulus. These are stuck to the skin, usually by means of double-sided adhesive tape, and the inner disk of skin is twisted while the torque required to achieve and maintain this rotation is monitored.[2] The probe of the twistometer consists of a torque motor and an angle sensor. The twistometer may also be configured as electromechanical oscillators connected to a spring exhibiting a variable degree of viscous recoil in the skin, in order to study the dynamic skin response.[3]

When the torque is applied for a given duration via the twistometer, the torque disk moves to a degree dependent on the compliance and viscosity of the tissue, and the resulting angular deformation is recorded. The creep

Table 13.1 Reported skin stiffness using uniaxial extensometers

Research group	Sites and conditions	Measured skin parameters and values
Manschot & Brakkee [55]	Human calf (along and across tibial axis)	Initial stiffness: 1 MPa (along axis), 0.15 MPa (across axis) Effective stiffness: 13 MPa (along axis), 4 MPa (across axis)
Clark *et al.* [4]	Human forearm	Skin stiffness: 0.75 N/mm
Quan *et al.* [5]	Human forearm and thigh (old and young)	Forearm skin stiffness: 1.92 N/mm (young), 2.86 N/mm (old) Thigh skin stiffness: 1.20 N/mm (young), 2.10 N/mm (old)

and relaxation behavior of skin in this test is similar to that obtained from a uniaxial extensometer. The difference between the two methods lies in the fact that the torsional device twists the skin through a small angle in all orientations, thus eliminating differences due to the test direction. With the twistometer, the deformations are applied in the plane of the skin to minimize the contribution of the deep layers. The stresses are applied in rotation, hence with an axis of symmetry. In contrast to uniaxial methods, the contribution of natural skin tensions can thus be averaged and the measurements are independent of the orientation of the imposed stress relative to the Langer's lines.

In the torsional test, a step torque instantaneously applied to the skin is maintained and then released to characterize creep and relaxation of the skin tissue. Typical skin deformation with time is depicted in Fig. 13.1. The parameter *Ue* is the elastic deformation of skin due to the application of an instantaneous load, *Uv* is the viscoelastic creep occurring after the elastic deformation, *Ur* is the elastic recovery, and *Uf* is the total extensibility.

Using a twistometer, Agache *et al.*[6] measured the skin deformation of 138 individuals from 3 to 89 years old and reported that the Young's modulus of the *in vivo* dermis was 0.42 MPa for the young age group and 0.85 MPa for the older age group. Boyce *et al.*[7] measured the deformation and recovery of skin after the treatment of burns with cultured skin substitutes, with the use of a dermal torque meter, in 10 patients. Assessments of burn scars

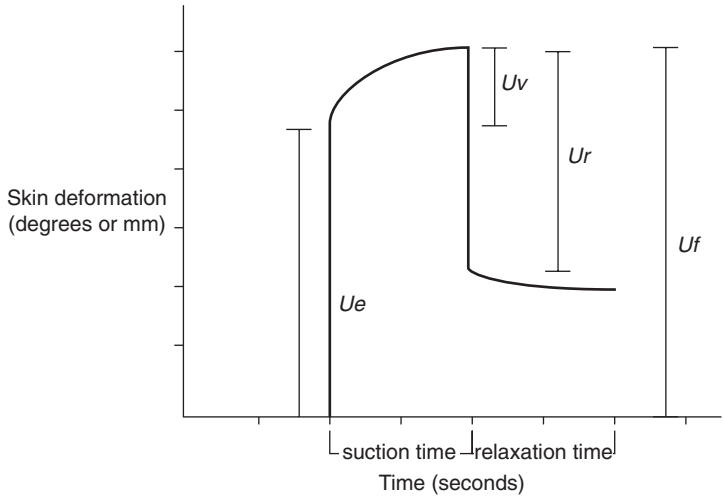

13.1 Graphical representations of the skin deformation–time curve under the mechanical testing of cutometer or twistometer. A suction force (torque for twistometer) is applied on the skin tissue and maintained during the suction time. The suction force is then released to characterize creep and relaxation.

reported time-dependent increases of skin extensibility and elastic recovery during the one-year post-treatment.

The torsional method can be used to determine the basic elastic and viscoelastic properties of skin and for the study of chronic sun exposure, racial differences in skin properties, scleroderma, and effects of cosmetic product application.

Cutometer: A skin pulling device called a cutometer has been used to quantify the mechanical behavior of skin under tension.[2] The device places a suction cup or cylinder perpendicularly on the skin surface and applies a negative pressure through the opening of a probe. The suction head is centered in the probe shield, with the diameter of the probe ranged from 2 to 8 mm, depending on the skin area.[3] The negative pressure is applied via a vacuum pump, which is incorporated with a pressure sensor. The resulting vertical deformation of the dome of the skin surface is measured by determining the depth of skin penetration into the probe. Skin elasticity parameters can be extracted from the applied pressure and the height of the skin dome. The typical skin deformation–time graph obtained is similar to the torsional test as depicted in Fig. 13.1. Cutometers usually provide the ability to alternate the pressure in a dynamic test mode to generate a cyclic suction such that the height of the raised skin can be recorded on each cycle.

The two most commonly used suction cup devices are the Dermaflex A (Department of Dermatology, Rishospital, Copenhagen, Denmark and the Institute of Technical Engineering (ATV), Glostrup, Denmark) and the DermaLab (Cortex Technology, Hadsund, Denmark).[3] These suction chamber devices are usually used to measure distensibility, elasticity and hysteresis of the tested skin.[8,9] Distensibility can be defined as the elevation of the skin under a particular tensile stress, and reflects the stiffness of the stretched skin. The stiffness is thought mainly to be due to the collagen fibers in the dermis. Elasticity defines the ability of the skin to recover from stress/stretch, which can be measured by monitoring the residual skin elevation after the first suction is terminated. Elasticity is also represented by *Ur*/*Uf*. The ability to regain the original shape following exposure to stretch seems to rely mainly on the elasticity fibers of the dermis. Hysteresis describes the irreversible alteration in maximum distensibility resulting from continuous cycles of stress applied on a particular area of the skin. It is determined from the difference between the elevation during the first cycle of suction and the last. Table 13.2 highlights some of the measured elastic parameters of skin using the cutometer, presented in the literature.

The cutometer has frequently been employed to help evaluate the effect of different pathological changes and treatment on skin elastic proper-

Table 13.2 Reported skin elastic parameters using cutometer

Research group	Sites and conditions	Measured skin elastic parameters and values
Jemec *et al.* [8]	Human palm and forearm	Distensibility: 1.76 mm (palm), 2.22 mm (forearm) Elasticity: 58% (palm), 68% (forearm) Hysteresis: 0.21 mm (palm), 0.20 mm (forearm)
Pedersen *et al.* [9]	Human forearm (sex and age)	Distensibility: 2.98 Elasticity: 90% Hysteresis: 0.18 mm Young's modulus: 5.26 MPa (Women), 4.8 MPa (Men) Young's modulus: 3.52 MPa (age 9–29), 4.77 MPa (age 30–39), 6.98 MPa (age 40–58)
Quan *et al.* [5]	Human forearm and thigh (old and young)	Forearm skin stiffness: 1.92 N/mm (young) 2.86 N/mm (old) Thigh skin stiffness: 1.20 N/mm (young) 2.10 N/mm (old)

ties.[10–14] Yoon *et al.*[14] quantified the facial skin elasticity in 96 diabetic patients and 83 normal subjects using a hand-held cutometer. The elasticity in the diabetics was significantly lower than in the non-diabetics. Using the cutometer, Dobrev[10] monitored the effect of therapy with dithranol by measuring the elasticity of 82 psoriatic plaques and of clinically uninvolved psoriatic skin in comparison with the skin of healthy controls. The plaques characterized significantly lower skin distensibility and elasticity compared with adjacent normal skin. After treatment, the mechanical parameters of psoriatic plaques approached the values of adjacent control skin. Van Zuijlen *et al.*[13] studied the effects of dermal substitution in acute burns and reconstructive surgery on skin elasticity measurements in 44 paired burn wounds and 44 paired scar reconstructions. The substituted scar reconstructions demonstrated an elasticity improvement of approximately 20% on a short-term basis but did not yield statistical evidence for a long-term clinical effectiveness of dermal substitution.

In terms of cosmetic skin treatment, Koch and Cheng[11] reported a significant increase of about 18.2% in skin elasticity after skin resurfacing using pulsed carbon dioxide lasers in 32 subjects, demonstrating its positive effect on skin-tightening. Pedersen and Jemec[12] studied the immediate plasticizing effect of water and glycerin on the skin of 23 healthy volunteers. Both water and glycerin were found to cause a significant increase in hysteresis with no significant difference in distensibility.

Indentation test (durometer, indentometer)

Durometer: The durometer is an indentometry device commonly used in the engineering industry to measure hardness of rubbers and other soft materials.[3] It has also been used to assess the degree of skin hardness to help quantify tissue hardness for prognostic and therapeutic reasons. The durometer reading was consistently higher for patients who were clinically judged to show greater induration. Durometry provides an easy to use and reproducible technique for measuring skin hardness on a linear scale. The instrument can thus serve as a standard noninvasive tool to measure skin hardness in systemic sclerosis or other dermatological diseases such as diabetic feet to assess skin involvement and to monitor the efficacy of treatment.

The first instrument used to assess skin hardness was a Rex durometer (model 1700, Rex Gauge Company, Inc., Glenview, IL).[3] This instrument is the international standard for measuring the hardness of rubber, plastic, nonmetallic materials, and soft tissue such as skin. It is a portable, hand-held device, which is provided with a calibrated gauge that registers linearly the relative degree of hardness (Shore hardness) on a scale of units divided from 0 to 100. This feature is the result of a spring-loaded interior that

ties.[10–14] Yoon *et al.*[14] quantified the facial skin elasticity in 96 diabetic patients and 83 normal subjects using a hand-held cutometer. The elasticity in the diabetics was significantly lower than in the non-diabetics. Using the cutometer, Dobrev[10] monitored the effect of therapy with dithranol by measuring the elasticity of 82 psoriatic plaques and of clinically uninvolved psoriatic skin in comparison with the skin of healthy controls. The plaques characterized significantly lower skin distensibility and elasticity compared with adjacent normal skin. After treatment, the mechanical parameters of psoriatic plaques approached the values of adjacent control skin. Van Zuijlen *et al.*[13] studied the effects of dermal substitution in acute burns and reconstructive surgery on skin elasticity measurements in 44 paired burn wounds and 44 paired scar reconstructions. The substituted scar reconstructions demonstrated an elasticity improvement of approximately 20% on a short-term basis but did not yield statistical evidence for a long-term clinical effectiveness of dermal substitution.

In terms of cosmetic skin treatment, Koch and Cheng[11] reported a significant increase of about 18.2% in skin elasticity after skin resurfacing using pulsed carbon dioxide lasers in 32 subjects, demonstrating its positive effect on skin-tightening. Pedersen and Jemec[12] studied the immediate plasticizing effect of water and glycerin on the skin of 23 healthy volunteers. Both water and glycerin were found to cause a significant increase in hysteresis with no significant difference in distensibility.

Indentation test (durometer, indentometer)

Durometer: The durometer is an indentometry device commonly used in the engineering industry to measure hardness of rubbers and other soft materials.[3] It has also been used to assess the degree of skin hardness to help quantify tissue hardness for prognostic and therapeutic reasons. The durometer reading was consistently higher for patients who were clinically judged to show greater induration. Durometry provides an easy to use and reproducible technique for measuring skin hardness on a linear scale. The instrument can thus serve as a standard noninvasive tool to measure skin hardness in systemic sclerosis or other dermatological diseases such as diabetic feet to assess skin involvement and to monitor the efficacy of treatment.

The first instrument used to assess skin hardness was a Rex durometer (model 1700, Rex Gauge Company, Inc., Glenview, IL).[3] This instrument is the international standard for measuring the hardness of rubber, plastic, nonmetallic materials, and soft tissue such as skin. It is a portable, hand-held device, which is provided with a calibrated gauge that registers linearly the relative degree of hardness (Shore hardness) on a scale of units divided from 0 to 100. This feature is the result of a spring-loaded interior that

senses hardness by applying an indentation load to the specimen via a retractable indentor.

Durometry measurements were found to be highly reproducible at the same site in each subject and in different clinical conditions.[3] However, durometer readings are insensitive in some skin areas, such as the forehead and dorsal digit, where subcutaneous tissue is less represented. The relative high stiffness of the underlying bone or tendon structure is suggested as a cause of failure of differentiation between normal and indurated skin tissue.

Romanelli and Falanga[15] measured the degree of skin induration in lipodermatosclerosis on the medial aspect of the leg, on 30 patients, with the use of a durometer. An increase in skin severity scores from 0 to 3 was found to correspond to an increasing durometer reading from 25 to 60. The durometer was suggested as an effective and reliable instrument for measuring skin hardness in patients with lipodermatosclerosis and venous ulceration, for the quantification of skin induration and ulcer healing. The noninvasive determination of skin hardness can be used to help identify patients at potential risk of developing neuropathic foot ulcers. Piaggesi *et al.*[16] evaluated the hardness of plantar skin in diabetic neuropathic feet of 36 patients by means of a durometer. Skin hardness was found to increase with the severity of diabetic neuropathy in patients. An increase in average skin stiffness from 41 (control) to 42 and 51, was measured for patients without and with diabetic neuropathy, respectively.

Recently, Thomas *et al.*[17] reported Shore hardness values ranging from 20 to 60 in different foot sole areas in diabetic subjects, depending on the severity of diabetic neuropathy. Using the Hayes formulation[18] (see page 231), they calculated the corresponding values of Young's modulus to hardness of foot sole soft tissue by measuring the indentation depth, the diameter of the indenter and the applied force. Shore values of 10, 20, 30, 60 and 90 were found to correspond to Young's moduli of 0.3, 0.84, 1.4, 3.85 and 7.9 MPa, respectively.

Indentometer: To obtain the compressive mechanical properties of the skin and underlying soft tissues, the majority of studies reported in literature have used indentation tests.[19–22] A number of indentation studies have been done to quantify the bulk soft tissue response of different regions of the body, using indentation devices of different technologies, such as linear variable differential transformers (LVDT) and ultrasound transducers, to measure the elasticity parameters.

Vannah and Childress[21] conducted an *in vivo* indentor test on the tissue stiffness of the calf of the lower leg, using a device consisting of an indentor with a linear variable differential transformer (LVDT) and a load cell. Prescribed displacement and resulting force were measured simultaneously

and the quantitative data of the nonlinear material stiffness and viscoelasticity occurring in the response of bulk soft tissue was applied for the design of soft tissue support. Zheng and Mak[23] developed a Tissue Ultrasound Palpation System (TUPS) which has a potential for clinical assessment of soft tissues over different regions. The pen-sized, hand-held probe consisted of an ultrasound transducer and a load cell connected in series. The thickness and deformation of the soft tissue layer during indentation were determined from the ultrasound echoes. The force response was monitored by a low profile load cell.

To extract Young's modulus from the force–indentation relationship, the formula developed by Hayes *et al.*[18] is often used. For a rigid, plane-ended and cylindrical indenter, the formula is

$$E = p(1 - \nu^2)/2aw_0\kappa(a/h,\ \nu) \qquad [13.1]$$

where E is the Young's modulus, p the load applied by the indenter, ν the Poisson's ratio, a the radius of the indenter, h the thickness of the measured layer, w_0 the depth of the indentation, and κ a geometric and material dependent factor.

A table of factor κ was given for several values of ratios of indenter radius to tissue layer thickness and the Poisson's ratio. Hayes' solution could be used to consider the layered effect and the lateral expansion of the soft tissue during indentation, based on the assumption of infinitesimal deformation and a frictionless indenter interface. Zhang *et al.*[24] investigated the influence of friction and large deformation during an indentation test of a layered material bonded to a rigid foundation using finite element analyses. Modified κ values were given[24] for the calculation of Young's modulus in the same manner as Hayes' solution, except that the results presented took into consideration the large deformation of the indented tissue and the friction at the skin/indenter interface.

An ultrasound indentation system is an effective tool for the assessment of soft tissue properties. The effective elastic modulus of the skin and subcutaneous tissues at different sites has been reported in the literature (Table 13.3).

Impact test (ballistometer)

The ballistometer employs a dynamic technique for assessing the intrinsic viscoelastic properties of skin.[3] The bulk soft tissue responses, involving contributions from the outermost skin layers to the underlying structures of fat, muscle, or bone, are documented. A lightweight hammer, anchored at one end, free-falls onto the tested skin surface under gravitational force; the resulting hammer oscillatory displacement–time data are recorded and associated physical parameters are determined.

Table 13.3 Reported skin stiffness from indentation tests

Research group	Tested sites	Young's modulus
Krouskop *et al.* [56]	Residual limbs	0.053 to 0.141 MPa
Torres-Moreno *et al.* [57]	Residual limbs	0.027 to 0.106 MPa
Mak *et al.* [20]	Residual limbs	0.021 to 0.194 MPa
Zheng *et al.* [58]	Forearms	0.014 to 0.059 MPa
Zheng and Mak, [59]	Limbs	0.0104 to 0.0892 MPa
Zheng *et al.* [60]	Plantar foot	0.043 to 0.118 MPa
Han *et al.* [61]	Breast	0.029 MPa

A ballistometer usually consists of a rotary transducer and magnet for holding and releasing the ballistic hammer at a fixed angle.[3] The hammer is assumed to be a rigid body, rotating about a noncentroidal axis and its motion can be represented by $\Sigma M_o = I_o\alpha$ where ΣM_o is the algebraic sum of the moments of the external forces about the axis of rotation (o), I_o is the moment of inertia of the hammer about the axis of rotation, and α is the angular acceleration of the hammer. The potential energy of the hammer can be calculated from the mass of the hammer, the distance from the center of rotation to the hammer's center of gravity, and the angular displacement of the hammer with respect to the test surface. The temporal angular velocity and angular acceleration of the hammer can be calculated from the measured angular displacement of the hammer. Alternatively, the angular velocity of the hammer at the instant of impact can be calculated from the conservation of kinetic and potential energy of the rotating hammer. The product of the hammer's moment of inertia and angular velocity is defined as the angular momentum of the hammer. The average force of the hammer during impact can be estimated from the change in angular momentum.

The ballistometer provides a noninvasive method for determining the viscoelastic properties of skin. The four parameters of common interests are amplitude, coefficient of restitution, cutaneous absorption coefficient and stiffness.[3] The amplitude, or angular displacement, measured with respect to the baseline is a measure of elasticity as it relates to the rebound energy of the skin. The coefficient of restitution is a measure of elasticity defined as the ratio between the hammer rebound speed to its speed just before impact on the skin. The coefficient of restitution is calculated either as the ratio of rebound and initial hammer speed or as the square root of the potential energy ratio of two adjacent peaks. The cutaneous absorption coefficient is another measure of elasticity, defined as a dynamic time constant, and presumes that the hammer impact energy is lost exponentially with time and is calculated from the peak height. The Cutaneous Absorption Coefficient, K is defined as

$$K = -(1/t_n)*log((AMP_n + BL)/(AMP_0 + BL)),$$

where t_n is the time at the nth peak, AMP refers to the angular displacement versus the baseline at the peak, and BL the baseline displacement from the horizontal or vertical. Skin stiffness is defined as the ratio of the hammer impact force to the skin deformation, that is the slope of the hammer impact force versus surface deformation curve.

The data obtained in a clinical study on 70 female subjects showed a decrease in the values with age for amplitude and the coefficient of restitution, while the cutaneous absorption coefficient shows a direct increase with age.[3] The stiffness value has an inverse relationship with age until the fourth to fifth decade, after which it increases sharply with age in females.

Using a ballistometer, Tosti *et al.*[25] studied the elastic properties of skin areas of 46 normal subjects ranging in age from 8 to 80 years, as well as on pathologic and cadaveric skin. The results showed a progressive decrease of coefficient of restitution with advancing age, as well as differences related to various skin regions. The tests performed on pathologic skin showed a lowered coefficient of restitution in epidermal hyperplasia, hyperkeratosis, sclerosis, and dermal infiltration. An increase of coefficient of restitution was observed when high water content was present in the skin.

13.3 Frictional properties of human skin

Frictional properties of human skin depend not only on the skin itself, such as its texture, its suppleness and smoothness, and its dryness or oiliness,[26] but also on its interaction with external surfaces and the outside environment. Investigation of skin frictional properties is relevant to several research fields, such as skin physiology, skin care products, textile and clothing industry, human friction-dependent activities and skin friction-induced injuries.

Frictional properties of skin surface may become an objective assessment of skin pathologies. It has been shown that frictional properties can reflect the chemical and physical properties of the skin surface and thus depend on the physiological variations as well as pathological conditions of skin.[26–30] The measurement of skin friction may be useful in studying the progress of individual skin disease.[28] Lodén *et al.*[27] found experimentally that the friction of skin with dry atopic subjects was significantly lower than that of the normal skin.

Skin frictional data have been used to evaluate skin care and cosmetic products.[31] Friction of skin forms an integral part of our tactile perception and plays an important role in the objective evaluation of consumer-perceptible skin attributes.[32,33] Some experiments[31,34–37] investigated friction changes induced by hydration and emollient application and the correlation with perceived skin feel.

Skin friction properties are also relevant to some friction-dependent functions, such as grasping, gripping and movement.[38–41] Such an understanding is very important in the design of handles, tools, controls and shoes. Bucholz *et al.*[42] investigated the frictional properties of human palmar skin to various materials, using a two-fingered pinch grip and effects of subjects, materials, moisture, pinch force. The investigation of the skin frictional properties is also helpful to understand the skin friction-induced injuries.[43–47] The injurious effects of friction on the skin and the underlying tissues can be divided into two classes, those without slip and those with slip. The former may rupture the epidermis and occlude blood and interstitial fluid flows by stretching or compressing the skin. The latter adds an abrasion to this damage. Research showed that the skin shear force produced by frictional force, combining with pressure is effective on occluding the skin blood flow.[48–50] Repetitive rubbing causes blistering and produces heat which may have uncomfortable and injurious consequences.

In lower-limb prosthetic socket and orthotic design, achieving a proper load transfer is the key issue since the soft tissues, such as those over residual limb, which are not suited for loading, have to support the body weight as well as other functional loads. Skin and prosthetic devices form a critical interface, at which skin friction is an important determinant on the mechanical interactional properties. Friction plays significant roles in supporting the load and in causing discomfort or skin damage.[51,52] To optimize frictional actions, there is a requirement to adequately understand the frictional properties between the skin and its contact surface. In textile and clothing industry, skin friction to the clothing materials is an important parameter for the correlation of sensation, comfort or fabric cling.[53]

Frictional properties between human skin and the prosthesis materials were measured using Measurement Technologies Skin Friction Meter (Aca-Derm Inc., California).[54] A spring balance was connected to a hand-held probe to monitor the normal force. An annular disk of the tested material was glued on the rotary end of the frictional meter. The probe sensing surface was annular with an outer diameter of 16 mm and an inner diameter of 10 mm. Five materials namely aluminum, nylon, silicone, sock cotton and Pelite were studied. Ten subjects without any skin problems participated in the study. The measurements were conducted at six anatomical sites, namely the dorsum of hand, palm of hand, anterior side of forearm, posterior side of forearm, anterior leg, posterior leg. The skin was untreated but clean. Various normal forces from 0.25 N to 1 N were applied. The frictional torques were measured at rotation speeds between 25 rpm to 62.5 rpm. Each test was repeated five times.

Tables 13.4 and 13.5 show the coefficients of friction over different sites and with different materials. In all the measurements, the coefficient of friction ranged from 0.24 to 0.65 and the average value for all the tested

Table 13.4 Coefficient of friction at the six anatomical sites (DH = dorsum of hand, PH = palm of hand, AF = anterior side of forearm, PF = posterior side of forearm, AL = anterior leg, PL = posterior leg)

Site	DH	PH	AF	PF	AL	PL
Coefficient	0.47 ± 0.12	0.62 ± 0.22	0.46 ± 0.10	0.43 ± 0.10	0.40 ± 0.10	0.40 ± 0.09

Table 13.5 Coefficient of friction with the five materials

Material	Al	Nylon	Silicone	Sock	Pelite
Coefficient	0.42 ± 0.14	0.37 ± 0.09	0.61 ± 0.21	0.51 ± 0.11	0.45 ± 0.07

Pelite = polyethylene foam

sites and materials was 0.41 ± 0.14. There was no significant difference in friction between the two anatomical sites measured. Among the five materials measured, silicone showed the highest coefficient of friction, and nylon showed the lowest.

13.4 Conclusion

Mechanical measurements of skin properties have progressed considerably in the past several decades. Reliable commercial devices are now available for measuring several different aspects of skin mechanics. With adequate control of the testing instruments, environment and specimens, it is possible to obtain valuable data relating to the effects of treatments, disease states, or the natural aging process. Because of the diversities of instrumental approaches and measured parameters, it is not feasible to set absolute standards for the experimental procedures. Rather, proper control of instrumental and testing parameters, measurement environment, and treatment site should be achieved in order to obtain reliable skin biomechanical measurements.

The noninvasive nature of available techniques provides effective methods for monitoring the temporal effects of disease, drugs, or cosmetics on *in vivo* skin. *In vitro* testing, on the other hand, provides repeatable standardized methods that can supply basic elastic and viscoelastic moduli for skin. Although interpretation of skin parameters measured *in vivo* is difficult, objective evaluations of the changes due to treatment or progress of disease, and the efficacy of competing treatments can be achieved. Measurement of skin mechanical properties is one important aspect of endeavor to help quantify and optimize different treatment modalities.

13.5 References

1. Lanir, Y. (1987). Skin Mechanics. In: *Handbook of Bioengineering*, Chapter 11, New York: McGraw-Hill.
2. Edwards, C. and Marks, R. (1995). Evaluation of biomechanical properties of human skin. *Clin Dermatol.*, **13**, 375–80.
3. Elsner, P. (2002). *Bioengineering of the skin: Skin biomechanics*, Boca Raton, Fla.: CRC Press.
4. Clark, J.A., Cheng, J.C. and Leung, K.S. (1996). Mechanical properties of normal skin and hypertrophic scars. *Burns*, **22**, 443–6.
5. Quan, M.B., Edwards, C. and Marks, R. (1997). Non-invasive *in vivo* techniques to differentiate photodamage and ageing in human skin. *Acta Derm. Venereol.*, **77**, 416–19.
6. Agache, P.G., Monneur, C., Leveque, J.L. and De Rigal, J. (1980). Mechanical properties and Young's modulus of human skin *in vivo*. *Arch. Dermatol. Res.*, **269**, 221–32.
7. Boyce, S.T., Supp, A.P., Wickett, R.R., Hoath, S.B. and Warden, G.D. (2000). Assessment with the dermal torque meter of skin pliability after treatment of burns with cultured skin substitutes. *J. Burn Care Rehabil.*, **21**, 55–63.
8. Jemec, G.B., Selvaag, E., Agren, M. and Wulf, H.C. (2001). Measurement of the mechanical properties of skin with ballistometer and suction cup. *Skin Res. Technol.*, **7**, 122–6.
9. Pedersen, L., Hansen, B. and Jemec, G.B. (2003). Mechanical properties of the skin: A comparison between two suction cup methods. *Skin Res. Technol.*, **9**, 111–15.
10. Dobrev, H. (2000). *In vivo* study of skin mechanical properties in psoriasis vulgaris. *Acta Derm Venereol.*, **80**, 263–6.
11. Koch, R.J. and Cheng, E.T. (1999). Quantification of skin elasticity changes associated with pulsed carbon dioxide laser skin resurfacing. *Arch. Facial Plast. Surg.*, **1**, 272–5.
12. Pedersen, L.K. and Jemec, G.B. (1999). Plasticising effect of water and glycerin on human skin *in vivo*. *J. Dermatol. Sci.*, **19**, 48–52.
13. van Zuijlen, P.P., Vloemans, J.F., van Trier, A.J., Suijker, M.H., van Unen, E., Groenevelt, F., Kreis, R.W. and Middelkoop, E. (2001). Dermal substitution in acute burns and reconstructive surgery: a subjective and objective long-term follow-up. *Plast. Reconstr. Surg.*, **108**, 1938–46.
14. Yoon, H.S., Baik, S.H. and Oh, C.H. (2002). Quantitative measurement of desquamation and skin elasticity in diabetic patients. *Skin Res. Technol.*, **8**, 250–4.
15. Romanelli, M. and Falanga, V. (1995). Use of a durometer to measure the degree of skin induration in lipodermatosclerosis. *J. Am. Acad. Dermatol.*, **32**, 188–91.
16. Piaggesi, A., Romanelli, M., Schipani, E., Campi, F., Magliaro, A., Baccetti, F. and Navalesi, R. (1999). Hardness of plantar skin in diabetic neuropathic feet. *J. Diabetes Complications*, **13**, 129–34.
17. Thomas, V.J., Patil, K.M. and Radhakrishnan, S. (2004). Three-dimensional stress analysis for the mechanics of plantar ulcers in diabetic neuropathy. *Med. Biol. Eng. Comput.*, **42**, 230–5.
18. Hayes, W.C., Keer L.M., Herrmann, G. and Mockros L.F. (1972). A mathematical analysis for indentation tests of articular cartilage. *J. Biomech.*, **5**, 541–51.

19. Reynolds, D.P. and Lord, M. (1992). Interface load analysis for computer-aided design of below-knee prosthetic sockets. *Med. Biol. Eng. Comput.*, **30**, 419–26.
20. Mak, A.F., Liu, G.H. and Lee, S.Y. (1994). Biomechanical assessment of below-knee residual limb tissue. *J. Rehabil. Res. Dev.*, **31**, 188–98.
21. Vannah, W.M. and Childress, D.S. (1996). Indentor tests and finite element modeling of bulk muscular tissue *in vivo*. *J. Rehabil. Res. Dev.*, **33**, 239–52.
22. Vannah, W.M., Drvaric, D.M., Hastings, J.A., Stand, J.A. 3rd. and Harning, D.M. (1999). A method of residual limb stiffness distribution measurement. *J. Rehabil Res. Dev.*, **36**, 1–7.
23. Zheng, Y.P. and Mak, A.F. (1996). An ultrasound indentation system for biomechanical properties assessment of soft tissues *in vivo*. *IEEE Trans. Biomed. Eng.*, **43**, 912–18.
24. Zhang, M., Zheng, Y.P. and Mak, A.F. (1997). Estimating the effective Young's modulus of soft tissues from indentation tests – Nonlinear finite element analysis of effects of friction and large deformation. *Med. Eng. Phys.*, **19**, 512–17.
25. Tosti, A., Compagno, G., Fazzini, M.L. and Villardita, S. (1977). A ballistometer for the study of the plasto-elastic properties of skin. *J. Invest. Dermatol.*, **69**, 315–17.
26. Lodén, M. (1995). Biophysical properties of dry atopic and normal skin with special reference to effects of skin care products. *ACTA Dermato-Venereologica* (suppl.)., **192**, 3–48.
27. Lodén, M., Olsson, H., Axell, T. and Werner, Y. (1992). Friction, capacitance and transepidermal water loss (TEWL) in dry atopic and normal skin. *Br. J. Dermatol.*, **126**, 137–41.
28. Comaish, J.S. and Bottoms, E. (1971). The skin and friction: Deviations from Amonotons' laws, and the effects of hydration and lubrication. *Br. J. Derm.*, **84**, 37–43.
29. Elsner, P., Wilhelm, D. and Maibach, H.I. (1990). Frictional properties of human forearm and vulvar skin: influence of age and correlation with transepidermal water loss and capacitance. *Dermatologica*, **181**, 88–91.
30. Cua, A.B., Wilhelm, K.P. and Maibach, H.I. (1995). Skin surface lipid and skin friction: Relation to age, sex and anatomical region. *Skin Pharmacol.*, **8**, 246–51.
31. El-Shimi, A.F. (1997). *In vivo* skin friction measurements. *J. Soc. Cosmet. Chem.*, **28**, 37–51.
32. Wolfram, L.J. (1983). Friction of skin. *J. Soc. Cosmet. Chem.*, **34**, 465–76.
33. Wolfram, L.J. (1989). Frictional properties of skin. In: *Cutaneous Investigation in Healthy and Disease Noninvasive Methods and Instrumentation*, edited by J. L. Leveque. New York: Marecel Dekker, 49–57.
34. Nacht, S., Close, J.A., Yeung, D. and Gans, E.H. (1981). Skin friction coefficient: Changes induced by skin hydration and emollient application and correlation with perceived skin feel. *J. Soc. Cosmet. Chem.*, **32**, 55–65.
35. Gerrard, W.A. (1987). Friction and other measurements of the skin surface. *Bioeng. Skin*, **3**, 123–39.
36. Hills, R.J., Unsworth, A. and Ive, F.A. (1994). A comparative study of the frictional properties of emollient bath additives using porcine skin. *Br. J. Dermat.*, **130**, 37–41.

37. Highley, D.R., Coomey, M., DenBeste, M. and Wolfram, L.J. (1977). Friction properties of skin. *J. Invest. Dermat.*, **69**, 303–5.
38. Cua, A.B., Wilhelm, K.P. and Maibach, H.I. (1990). Frictional properties of human skin: Relation to age, sex and anatomical region, stratum corneum hydration and transepidermal water loss. *Br. J. Derm.*, **123**, 473–79.
39. Johansson, R.S. and Cole, K.J. (1994). Grasp stability during manipulative actions. *Can. J. Physiol. Pharmacol.*, **72**, 511–24.
40. Smith, A.M. and Scott, S.H. (1996). Subjective scaling smooth surface friction. *J. Neurophysiology*, **75**, 1957–62.
41. Taylor, M.M. and Lenderman, S.J. (1975). Tactile roughness of grooved surfaces: A model and the effect of friction. *Perception and Psychophysics*, **17**, 23–36.
42. Buchholz, B., Frederick, L.J. and Armstrong, T.J. (1988). An investigation of human palmar skin friction and the effects of materials, pinch force and moisture. *Ergonomics*, **31**(3), 317–25.
43. Naylor, P.F.D. (1955). The skin surface and friction. *Br. J. Derm.*, **67**, 239–48.
44. Sulzberger, M.B., Cortese, T., Fishman, L. and Wiley, H.S. (1966). Studies on blisters produced by friction – I. Results of linear rubbing and twisting technics. *J. Invest. Dermatol.*, **47**, 56–65.
45. Dalton, B. (1982). Friction, intermitted or otherwise, the exciting cause of corns and callouses. *Chiropodist*, **37**, 372–80.
46. Armstrong, T.J. (1985). Mechanical consideration of skin in work. *Am. J. Industrial Med.*, **8**, 463–72.
47. Akers, C.W.A. (1985). Measurements of friction injuries in man. *Am. J. Industrial Med.*, **8**, 473–81.
48. Bennett, L., Kavner, D., Lee, B.K. and Frieda, A. (1979). Shear vs pressure as causative factors in skin blood flow occlusion. *Arch. Phy. Med. Rehabil.*, **60**, 309–14.
49. Zhang, M. and Roberts, V.C. (1993). The effect of shear forces externally applied to skin surface on underlying tissues. *J. Biomed. Eng.*, **15**, 451–6.
50. Zhang, M., Turner-Smith, A.R. and Roberts, V.C. (1994). The reaction of skin and soft tissue to shear forces applied externally to the skin surface. *J. of Eng. in Medicine*, **208**, 217–22.
51. Zhang, M., Lord, M., Turner-Smith, A.R. and Roberts, V.C. (1995). Development of a non-linear finite element modelling of the below-knee prosthetic socket interface. *Med. Eng. Phys.*, **17**, 559–66.
52. Zhang, M., Turner-Smith, A.R., Tanner, A. and Roberts, V.C. (1996). Frictional action at residual limb/prosthetic socket interface. *Med. Eng. Phys.*, **18**, 207–214.
53. Kenins, P. (1994). Influence of fiber type and moisture on measured fabric-to-skin friction. *Textile Res. J.*, **64**, 722–8.
54. Zhang, M. and Mak, A.F. (1999). *In vivo* friction properties of human skin. *Prosthet. Orthot. Int.*, **23**, 135–41.
55. Manschot, J.F. and Brakkee, A.J. (1986). The measurement and modelling of the mechanical properties of human skin *in vivo* – I. The measurement. *J. Biomech.*, **19**, 511–15.
56. Krouskop, T.A., Dougherty, D.R. and Vinson, F.S. (1987). A pulsed Doppler ultrasonic system for making noninvasive measurements of the mechanical properties of soft tissue. *J. Rehabil. Res. Dev.*, **24**, 1–8.

57. Torres-Moreno, R., Saunders, C.G., Foort, J. and Morrison, J.B. (1991). Computer-aided design and manufacture of an above-knee amputee socket. *J. Biomed. Eng.*, **13**, 3–9.
58. Zheng, Y., Mak, A.F. and Lue, B. (1999). Objective assessment of limb tissue elasticity: development of a manual indentation procedure. *J. Rehabil. Res. Dev.*, **36**, 71–85.
59. Zheng, Y.P. and Mak, A.F. (1999). Effective elastic properties for lower limb soft tissues from manual indentation experiment. *IEEE Trans. Rehabil. Eng.*, **7**, 257–67.
60. Zheng, Y.P., Choi, Y.K., Wong, K., Chan, S. and Mak, A.F. (2000). Biomechanical assessment of plantar foot tissue in diabetic patients using an ultrasound indentation system. *Ultrasound Med. Biol.*, **26**, 451–6.
61. Han, L., Noble, J.A. and Burcher, M. (2003). A novel ultrasound indentation system for measuring biomechanical properties of *in vivo* soft tissue. *Ultrasound Med Biol.*, **29**, 813–23.